N65-88354

SPACE TECHNOLOGY LABORATORIES, INC.
A SUBSIDIARY OF THOMPSON RAMO WOOLDRIDGE INC.
SPACE TECHNOLOGY CENTER · ONE SPACE PARK · REDONDO BEACH, CALIFORNIA

SPACE TECHNOLOGY LABORATORIES, INC.
No. One Space Park
Redondo Beach, California

A STUDY OF THE CONTROL AND DYNAMIC STABILITY OF THE SATURN C-1 CONFIGURATION

Final Report

Volume III. Technical Data

20 April 1962

Report No. 8620-6002-RU-000

Contract No. NAS 8-1624

Prepared for

GEORGE C. MARSHALL SPACE FLIGHT CENTER
Huntsville, Alabama

TABLE OF CONTENTS

ILLUSTRATIONS

1. INTRODUCTION

This report is the result of Task 1 of Contract NAS 8-1624, "Study of the Control and Dynamic Stability problem of the Saturn Space Vehicle, Especially the C-1 Configuration". This task was to prepare a detailed technical description of the missile configuration which was studied and the description is given in this report.

Definitions of the symbols used in the report are given in Section 2. Some of these symbols are also defined in Figures 2, 3, 8 and 9 which show the coordinate systems and missile geometry conventions used. Section 3 contains the basic parameters of the missile configuration as specified by Marshall Space Flight Center. These basic parameters were used to compute the parameters given in Sections 4 and 5. Section 4 contains the coordinate system, equations, computed coefficients, and computer diagrams used in the analysis of the adaptive angle-of-attack control system described in Volume II. This analysis consists of a time-variable two-dimensional analog simulation to establish the performance capability of this control system. Section 5 contains the coordinate system, equations, computed parameters and computer diagrams used in the evaluation of the performance of the adaptive digital bending compensator described in Volume I. For this purpose, a digital-analog combined simulation study was performed using a time-invariant, two-dimensional simulation of the missile system.

2. GLOSSARY OF SYMBOLS

A	Aerodynamic reference area
A_i	Acceleration indicated by accelerometer
a_x, a_y	Acceleration components of the total center of gravity
a_o	Autopilot inertial attitude gain
a_1	Autopilot inertial attitude - rate gain
b_o	Autopilot angle-of-attack gain
C_1	Aerodynamic restoring torque coefficient
C_2	Control torque coefficient
C_{N_α}	Normal force coefficient slope with respect to angle-of-attack
c.g.1	Center of gravity of missile
c.g.2	Center of gravity of missile exclusive of deflected engines and sloshing propellants
c.g.3	Center of gravity of missile exclusive of sloshing propellants
D	Aerodynamic axial drag
f_i	Frequency of the i^{th} slosh mode
g	Acceleration due to gravity
h	Missile altitude
I_1	Moment of inertia of missile about c.g.1
I_3	Moment of inertia of missile exclusive of sloshing propellants about c.g.3
I_n	Moment of inertia of deflected engines about gimbal point
K_I	Control loop integral gain
k	Adaptive loop output $\left(\frac{b_o}{a_o + b_o}\right)$
l_1	Distance from gimbal to c.g.1
l_3	Distance from gimbal to c.g.3
l_n	Distance from gimbal to engine c.g.

l_p	Distance between center of pressure and total center of gravity
M_1	Mass of missile
M_2	Mass of missile exclusive of deflected engines and sloshing propellants
M_3	Mass of missile exclusive of sloshing propellants
m_F	Mass of sloshing liquid in booster stage
m_L	Mass of sloshing liquid in second stage
m_i	Modal mass of the i^{th} bending mode
m_n	Mass of deflected engines
N'	Normal force per unit angle of attack
q	Dynamic pressure
q_i	Generalized i^{th} mode bending coordinate
R'	Control force per unit of control deflection
r	Radial location of control motors from missile centerline
s	Laplace operator
T	Thrust of eight engines
V	Inertial velocity of c.g.2
v	Deflection of the average missile centerline due to an engine deflection
V_R	Velocity of c.g.2 relative to wind
V_W	Wind component normal to reference trajectory
w	Rotation of the average missile centerline due to an engine deflection
$\bar{x}_i$	Distance from c.g. to i^{th} sloshing mass attach point
Z_B	Direction perpendicular to missile centerline
Z_{B_3}	Direction perpendicular to missile centerline extending from c.g.3
Z_T	Direction perpendicular to reference trajectory
Z_{T_g}	Direction perpendicular to reference trajectory extending from guidance compartment

α	Aerodynamic angle of attack
α_i	Angle of attack indicated by angle-of-attack meter
α_w	Angle of attack due to wind
β	Cant of outboard motors
β_{id}	Angle required to cant outboard motors through c.g.1
γ_o	Path angle
γ_1	Tilt angle
δ	Control deflection angle
δ_a	Engine actuator output
δ_c	Engine actuator command input
ζ_A	Accelerometer damping ratio
ζ_F	Damping ratio of booster stage slosh mode
ζ_L	Damping ratio of second stage slosh mode
ζ_R	Rate gyro damping ratio
ζ_{AE}	Angle-of-attack meter aerodynamic damping ratio
ζ_{ME}	Angle-of-attack meter mechanical damping ratio
ζ_a	Actuator damping ratio
ζ_i	Damping of the i^{th} bending mode
ζ_n	Engine damping ratio
θ	Attitude angle
θ_P	Position gyro output
$\dot{\theta}_R$	Rate gyro output
λ_F	Displacement of booster stage sloshing mass from missile centerline
λ_L	Displacement of second stage sloshing mass from missile centerline
μ_i	Ratio of i^{th} sloshing mass to total missile mass
μ_T	Deflection at the engine gimbal station
	[illegible]

ξ	Missile station measured from base
ξ_1	Station of c.g.1
ξ_2	Station of c.g.2
ξ_3	Station of c.g.3
ξ_A	Station of accelerometer
ξ_F	Station of booster stage slosh spring attachment point
ξ_L	Station of second stage slosh spring attachment point
ξ_P	Station of position gyro
ξ_R	Station of rate gyro
ξ_T	Station of gimbal
ξ_{cp}	Station of aerodynamic center of pressure
ξ_α	Station of angle-of-attack meter
τ_p	Time constant of the demodulator
$\phi_i(\xi)$	Normalized deflection of the i^{th} bending mode at Station ξ
$\phi'_i(\xi)$	Normalized slope of the i^{th} bending mode at Station ξ
ψ	Angle between inertial velocity vector and missile centerline
ψ_T	Slope at the engine gimbal station
ω_A	Accelerometer natural frequency
ω_F	Booster stage slosh mode natural frequency
ω_L	Second stage slosh mode natural frequency
ω_R	Rate gyro natural frequency
ω_a	Actuator natural frequency
ω_i	Frequency of the i^{th} bending mode
ω_n	Engine natural frequency
ω_α	Angle-of-attack meter natural frequency

Q_i	Bending coordinate for the i^{th} mode with control engines removed
θ_ϵ	Control system error signal
φ_i	Deflection of the i^{th} bending mode of missile with control engines removed
φ'_i	Slope of the i^{th} bending mode of missile with control engines removed
Ω_i	Frequency of the i^{th} mode of missile with control engines removed

3. BASIC PARAMETERS

This section contains the basic parameters of the missile configuration as specified by the Marshall Space Flight Center. These basic parameters were used to compute the parameters found in Sections 4 and 5. Included in this section are a table of the parameters that remain constant throughout the booster flight, a table of the time variable parameters at seventeen times of flight for an all-engines-burning trajectory, a table of fluid-slosh parameters at four times of flight, and structural-modes parameters. The wind profiles suggested by MSFC for use in evaluating control system response to wind disturbances are shown in Figure 1. These profiles were constructed from data given in Reference 1.

3.1 Table of Constant Parameters

A	33.467522	m^2
g	9.79	m/sec^2
I_n	318.54	$kg\text{-}m\text{-}sec^2$
l_n	0.68603	m
m_L	2647.2183	$kg\text{-}sec^2/m$
m_F	1156.1508	$kg\text{-}sec^2/m$
m_n	298.34	$kg\text{-}sec^2/m$
r	2.413	m
β	6.0	deg
$\delta_{a\ max}$	7	deg
$\dot{\delta}_{a\ max}$	15	deg/sec
ζ_A	0.7	
ζ_R	0.7	
ζ_{AE}	0.05	
ζ_{ME}	0.15	

Table of Constant Parameters (continued)

ζ_a	0.966	
ζ_n	0.07	
ξ_A	1630	in
ξ_P (preferred)	1630	in
ξ_R (preferred)	950	in
ξ_T	100	in
ξ_α	1800	in
τ_p	1/282.6	sec
ω_A	56.55	rad/sec
ω_R	188.5	rad/sec
ω_a	34.5	rad/sec
ω_n	62.83	rad/sec
ω_α	251	rad/sec

3.2 Table of Variable Parameters - All Engines Burning

Time sec	I_1 kg sec² m	M_1 kg sec²/m	T kg	D kg	R' kg	C_{N_α}	(T-D)/M_1 m/sec²
0	2.51×10^6	45879	596690	0	298345	2.00	13.0
10	2.45×10^6	43395	598530	2690	299265	2.00	13.7
20	2.40×10^6	41033	603980	6218	301990	2.00	14.6
30	2.37×10^6	38610	613430	9554	306715	2.00	15.6
40	2.35×10^6	36187	626250	16902	313125	2.02	16.8
50	2.35×10^6	33764	641000	42541	320500	2.07	17.7
60	2.35×10^6	31342	655400	81700	327700	2.13	18.3
67	2.34×10^6	29646	664113	78340	332057	2.25	19.8
70	2.33×10^6	28919	667320	68789	333660	2.30	20.7
80	2.32×10^6	26496	675290	44325	337645	2.61	23.8
90	2.30×10^6	24073	679810	24085	339905	3.02	27.2
100	2.28×10^6	21651	681990	11139	340995	3.37	31.0
110	2.22×10^6	19228	682860	4543	341430	3.51	35.3
120	2.07×10^6	16805	683170	1770	341585	3.47	40.6
130	1.84×10^6	14382	683270	629	341635	3.29	47.5
138.9	1.58×10^6	12216	683310	209	341655	2.80	55.9
144.9	1.45×10^6	11489	341660	83	170830	2.67	29.7

Time sec	V m/sec	h km	q kg/m^2	ξ_1 m	ξ_{cp} m	γ_o deg	γ_1 deg
0	.0000	.0000	.0000	14.8775	36.4846	.0000	.0000
10	36	.2	82	14.6164	36.4846	.0000	.1
20	77.0	.7	360	14.4206	36.4846	2.2	2.5
30	132	1.8	911	14.1595	36.4846	6.6	7.0
40	198	3.4	1738	14.0289	36.4193	12.6	13.1
50	277	5.7	2684	13.95365	36.2887	19.3	19.3
60	365	8.6	3325	13.8984	35.9623	26.0	26.0
67	438	11.1	3524	13.8331	35.5054	30.6	30.7
70	473	12.2	3435	13.8984	35.1795	32.6	32.6
80	616	16.6	2923	14.0289	33.9387	38.6	38.6
90	798	21.9	2143	14.2900	32.6984	43.8	43.9
100	1021	28.2	1274	14.6164	31.7193	48.2	[illegible]
110	1290	35.6	645	15.3345	31.1318	51.8	52.1
120	1610	44.2	298	16.4442	31.1318	54.2	55.1
130	1995	54.2	135	18.0762	31.3276	57.2	57.7
138.9	2410	64.5	61	19.8387	32.3720	59.0	59.4
144.9	2553	72.1	25	20.6220	32.8290	60.0	59.4

3.3 Table of Fluid-Slosh Parameters

		0 sec	40 sec	80 sec	120 sec
$\bar{x}_1$	m	- 3.45	- .06	4.57	12.02
$\bar{x}_2$	m	- 4.10	- .62	3.96	11.87
$\bar{x}_3$	m	- 3.93	- .49	3.94	11.69
$\bar{x}_4$	m	- 8.41	-9.28	--9.08	- 5.16
$\bar{x}_5$	m	-11.81	-12.68	-12.48	- 8.56
μ_1		.0086	.0114	.0166	.0225
μ_2		.0097	.0128	.0187	.0304
μ_3		.0069	.0091	.0132	.0213
μ_4		.0577	.0761	.1109	.2039
μ_5		.0042	.0056	.0081	.0149
f_1	cps	.719	.813	1.030	1.216
f_2	cps	.880	.995	1.260	1.633
f_3	cps	.880	.995	1.260	1.633
f_4	cps	423	.479	.606	.832
f_5	cps	.495	.560	.708	.974

$i = 1$ 105 in. Tank

$i = 2$ 70 in. Lox

$i = 3$ 70 in. Fuel

$i = 4$ Second stage Lox

$i = 5$ Second stage LH_2

3.4 Structural-Modes Parameters

First Mode

Station	Liftoff		Max Q		Cutoff	
	Mode Deflection	Mode Slope	Mode Deflection	Mode Slope	Mode Deflection	Mode Slope
in		in^{-1}		in^{-1}		in^{-1}
0	.250	.00070	.255	.00090	.250	.00093
50	.210	.00070	.210	.00094	.215	.00094
100	.175	.00070	.170	.00095	.170	.00094
150	.140	.00070	.125	.00094	.120	.00092
200	.110	.00070	.085	.00092	.080	.00091
250	.075	.00070	.045	.00090	.030	.00088
300	.045	.00069	.010	.00086	-.010	.00084
350	.015	.00066	-.030	.00082	-.050	.00080
400	-.015	.00061	-.070	.00076	-.090	.00075
450	-.045	.00056	-.100	.00069	-.120	.00069
500	-.075	.00048	-.135	.00060	-.155	.00062
550	-.103	.00040	-.160	.00052	-.185	.00055
600	-.130	.00030	-.190	.00044	-.210	.00046
650	-.145	.00020	-.215	.00034	-.235	.00036
700	-.150	.00008	-.230	.00023	-.250	.00026
750	-.145	-.00005	-.240	.00012	-.260	.00015
800	-.140	-.00020	-.240	0	-.265	.00003
850	-.120	-.00034	-.235	-.00017	-.260	-.00010
900	-.095	-.00047	-.220	-.00036	-.255	-.00024
950	-.070	-.00059	-.200	-.00056	-.240	-.00039
1000	-.030	-.00071	-.175	-.00070	-.220	-.00052
1050	+.010	-.00080	-.140	-.00081	-.190	-.00065
1100	.050	-.00088	-.110	-.00091	-.160	-.00077
1150	.090	-.00093	-.100	-.00098	-.120	-.00088
1200	.135	-.00098	-.060	-.00104	-.080	-.00098
1250	.185	-.00100	+.015	-.00109	-.040	-.00103
1300	.235	-.00104	.085	-.00114	+.010	-.00108
1350	.285	-.00108	.145	-.00120	.070	-.00118
1400	.340	-.00112	.220	-.00124	.130	-.00130
1450	.400	-.00115	.280	-.00129	.200	-.00140
1500	.455	-.00118	.350	-.00134	.280	-.00148
1550	.515	-.00121	.420	-.00139	.355	-.00156

First Mode

(continued)

Station in	Liftoff Mode Deflection	Liftoff Mode Slope in^{-1}	Max Q Mode Deflection	Max Q Mode Slope in^{-1}	Cutoff Mode Deflection	Cutoff Mode Slope in^{-1}
1600	.575	-.00123	.485	-.00143	.430	-.00160
1650	.630	-.00124	.540	-.00146	.505	-.00164
1700	.695	-.00125	.635	-.00148	.585	-.00168
1750	.755	-.00126	.710	-.00150	.665	-.00168
1800	.810	-.00126	.780	-.00151	.750	-.00168
1850	.880	-.00126	.860	-.00151	.830	-.00168
1900	.950	-.00125	.940	-.00148	.915	-.00165
1940	1.000	-.00124	1.000	-.00146	1.000	-.00164

Time	Frequency	Modal Mass
Liftoff	1.6318 cps	61.87 lb sec^2/in
Max Q	2.0925 cps	48.21 lb sec^2/in
Cutoff	2.5601 cps	35.20 lb sec^2/in

$$\zeta_1 = 0.005$$

Second Mode

Station	Liftoff		Max Q		Cutoff	
	Mode Deflection	Mode Slope	Mode Deflection	Mode Slope	Mode Deflection	Mode Slope
in		in^{-1}		in^{-1}		in^{-1}
0	-.2	-.0009	-.36	-.00156	-.40	-.00268
50	-.16	-.0009	-.29	-.0016	-.28	-.00274
100	-.12	-.0009	-.20	-.0016	-.13	-.00270
150	-.08	-.00088	-.12	-.0015	.00	-.00262
200	-.03	-.00084	-.05	-.00156	+.12	-.00250
250	.01	-.00078	+.02	-.0014	.24	-.00232
300	.04	-.00070	.06	-.0012	.34	-.00210
350	.075	-.00060	.14	-.00108	.42	-.00186
400	.095	-.00048	.18	-.00085	.50	-.00158
450	.11	-.00035	.21	-.0006	.57	-.00128
500	.12	-.0002	.23	-.0003	.67	-.00096
550	.12	.00000	.24	-.00002	.69	-.00059
600	.115	.00020	.24	.00022	.69	-.00025
650	.10	.00042	.22	.00045	.69	+.00010
700	.08	.00061	.19	.00062	.68	.00045
750	.055	.00072	.18	.00078	.65	.00084
800	.02	.00076	.11	.00088	.60	.0012
850	-.02	.00074	.05	.00096	.52	.0015
900	-.06	.00068	.00	.0010	.44	.0018
950	-.10	.00065	-.06	.00104	.33	.0035
1000	-.155	.00068	-.11	.00115	.21	.00270
1050	-.20	.00070	-.14	.00116	.05	.00284
1100	-.23	.0006	-.20	.0010	-.09	.00278
1150	-.245	-.00010	-.22	.00005	-.18	.0019
1200	-.24	-.00092	-.24	-.00017	-.25	.00115
1250	-.215	-.00066	-.23	-.0003	-.29	.00072
1300	-.18	-.00088	-.18	-.0005	-.32	.0004
1350	-.14	-.0011	-.17	-.0007	-.33	.0000
1400	-.09	-.0013	-.13	-.0011	-.31	-.0006
1450	-.02	-.0015	-.08	-.0015	-.27	-.00125
1500	+.05	-.0017	.00	-.00168	-.20	-.00162
1550	.14	-.00185	+.08	-.0018	-.10	-.0020

Second Mode
(continued)

Station	Liftoff		Max Q		Cutoff	
	Mode Deflection	Mode Slope	Mode Deflection	Mode Slope	Mode Deflection	Mode Slope
in		in^{-1}		in^{-1}		in^{-1}
1600	.24	-.00201	+.20	-.0033	+.02	-.0023
1650	.34	-.00212	+.31	-.00235	.16	-.0026
1700	.46	-.00218	+.42	-.00235	.28	-.00285
1750	.57	-.00220	+.54	-.0024	.42	-.00298
1800	.68	-.00221	+.66	-.0024	.56	-.00300
1850	.80	-.00221	+.77	-.0024	.70	-.00297
1900	.90	-.00220	+.9	-.00235	.85	-.00288
1940	1.00	-.00218	1.0	-.0023	1.00	-.00276

Time	Frequency	Modal Mass
Liftoff	4.5513 cps	37.82 lb sec^2/in
Max Q	4.9971 cps	48.096 lb sec^2/in
Cutoff	7.2035 cps	57.173 lb sec^2/in

$$\zeta_2 = 0.005$$

Third Mode

Station	Liftoff		Max Q		Cutoff	
	Mode Deflection	Mode Slope	Mode Deflection	Mode Slope	Mode Deflection	Mode Slope
in		in^{-1}		in^{-1}		in^{-1}
0	1.05	.0064	1.020	.00608	.7	.00541
50	1.0	.0066	1.000	.00629	.41	.00575
100	.65	.00658	.750	.00632	.204	.00568
150	.385	.00644	.470	.00617	-.065	.00518
200	.125	.00609	0	.00575	-.425	.00400
250	-.12	.00516	-.225	.00390	-.570	.00256
300	-.35	.00372	-.335	.00260	-.645	.00134
350	-.50	.00328	-.400	.00156	-.670	.00030
400	-.58	.00292	-.430	.00016	-.665	-.000544
450	-.59	.00244	-.430	-.00160	-.625	-.00130
500	-.555	-.00156	-.345	-.00250	-.560	-.00198
550	-.445	-.00238	-.210	-.00295	-.455	-.00246
600	-.29	-.00304	-.070	-.00318	-.325	-.00271
650	-.053	-.00332	+.10	-.00311	-.190	-.00274
700	.110	-.00332	.285	-.00300	-.06	-.00266
750	.210	-.00256	.435	-.00262	.06	-.00242
800	.250	-.00088	.50	-.00168	.17	-.00209
850	.260	-.00022	.520	.00010	.27	-.00159
900	.245	+.00042	.500	.00086	.34	-.00090
950	.210	.00120	.440	.00176	.35	-.00001
1000	.135	.00264	.335	.00314	.32	.00088
1050	0	.00288	.150	.00360	.26	.00180
1100	-.205	.00270	-.065	.00350	.17	.00280
1150	-.290	.00100	-.205	.00194	.055	.00342
1200	-.335	.00064	-.305	.00134	-.075	.00348
1250	-.355	.00042	-.370	.00102	-.21	.00306
1300	-.355	.00010	-.408	.00070	-.35	.00211
1350	-.345	-.00030	-.42	.00028	-.485	.00140
1400	-.320	-.00086	-.405	-.000328	-.550	.00072
1450	-.285	-.00137	-.360	-.00121	-.560	.00006
1500	-.230	-.00182	-.290	-.00197	-.540	-.00060
1550	-.160	-.00219	-.185	-.00242	-.490	-.00128

Third Mode
(continued)

	Liftoff		Max Q		Cutoff	
Station in	Mode Deflection	Mode Slope in^{-1}	Mode Deflection	Mode Slope in^{-1}	Mode Deflection	Mode Slope in^{-1}
1600	-.06	-.00249	-.075	-.00274	-.380	-.00203
1650	.09	-.00272	.055	-.00305	-.220	-.00288
1700	.28	-.00287	.19	-.00314	-.045	-.00400
1750	.455	-.00296	.34	-.00323	+.135	-.00447
1800	.615	-.00298	.51	-.00328	.335	-.00464
1850	.770	-.00296	.685	-.00326	.54	-.00461
1900	.905	-.00285	.88	-.00318	.79	-.00440
1940	1.00	-.00269	1.00	-.00301	1.0	-.00390

Time	Frequency	Modal Mass
Liftoff	7.0375 cps	274.43 lb sec^2/in
Max Q	8.1376 cps	226.03 lb sec^2/in
Cutoff	13.7366 cps	59.933 lb sec^2/in

$\zeta_3 = 0.005$

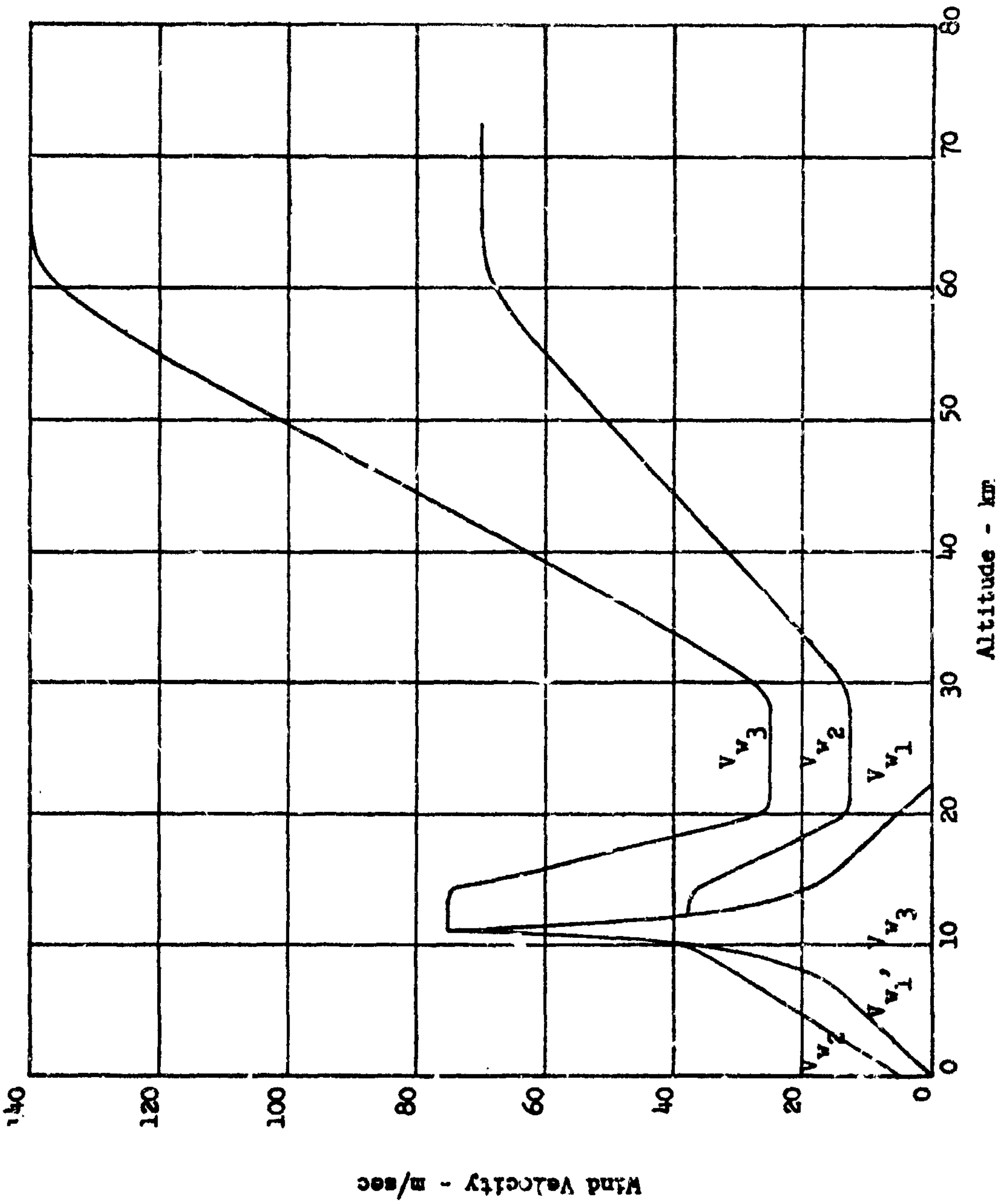

Figure 1
Wind Speed vs. Altitude Profiles

4. ADAPTIVE ANGLE-OF-ATTACK STUDY

This section contains the equations and computed coefficients for use in the study of the adaptive angle-of-attack control system The coordinate system and missile geometry conventions used are shown in Figures 2 and 3.

The information for this study is divided into two sections, that for the digital analysis and that for the analog computer simulation. Section 4.1 contains a discussion of the assumptions made and the effects included in the digital analysis.

Section 4.2 contains a discussion of the assumptions made and the effects included in the analog computer simulation of the missile dynamics. This is followed by a list of the equations and diagrams of the computer mechanizations for use in the simulation. The remainder of this section contains the computed coefficients for use in the computer simulation.

4.1 Digital Analysis

The equations and computed coefficients for use in the digital analysis of the angle-of-attack control system are presented in this section. The purpose of this analysis is to choose the control system gains that used in the analog computer simulation and to obtain frequency response and transient response data to be used to check the analog computer simulation.

The coefficients for this analysis were computed at three times of flight corresponding to the time when the angle-of-attack feedback loop would be closed, the time when maximum dynamic pressure occurs, and the time when maximum system gain occurs. In using the equations in this section, an attempt was made to include all linear terms consistent with the following assumptions:

1. All physical parameters of the missile such as mass, inertia, and thrust are considered constant.

2. Aerodynamic forces are assumed to vary linearly with the total angle of attack developed by the centerline of the missile.

3. The dynamic equations are for motions in the missile yaw plane. The trim conditions on α, θ, and δ will be zero in this plane. The equations are also applicable to the pitch plane if the trimmed values of these variables may be neglected.

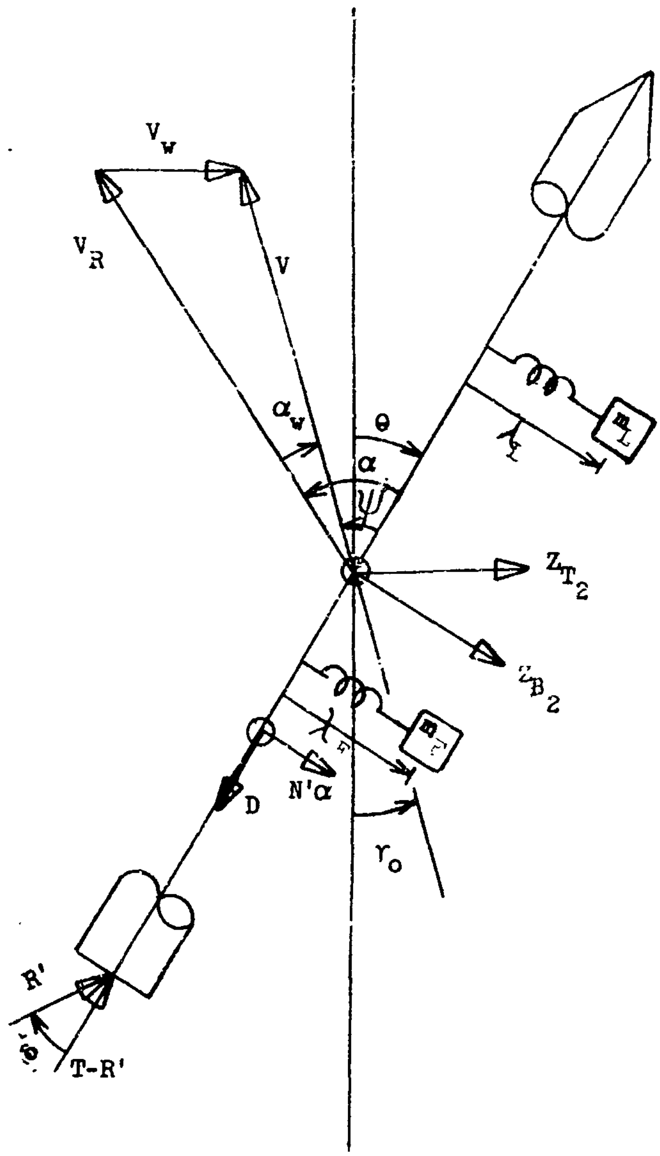

Figure 2

Coordinate System for Angle-of-Attack Study

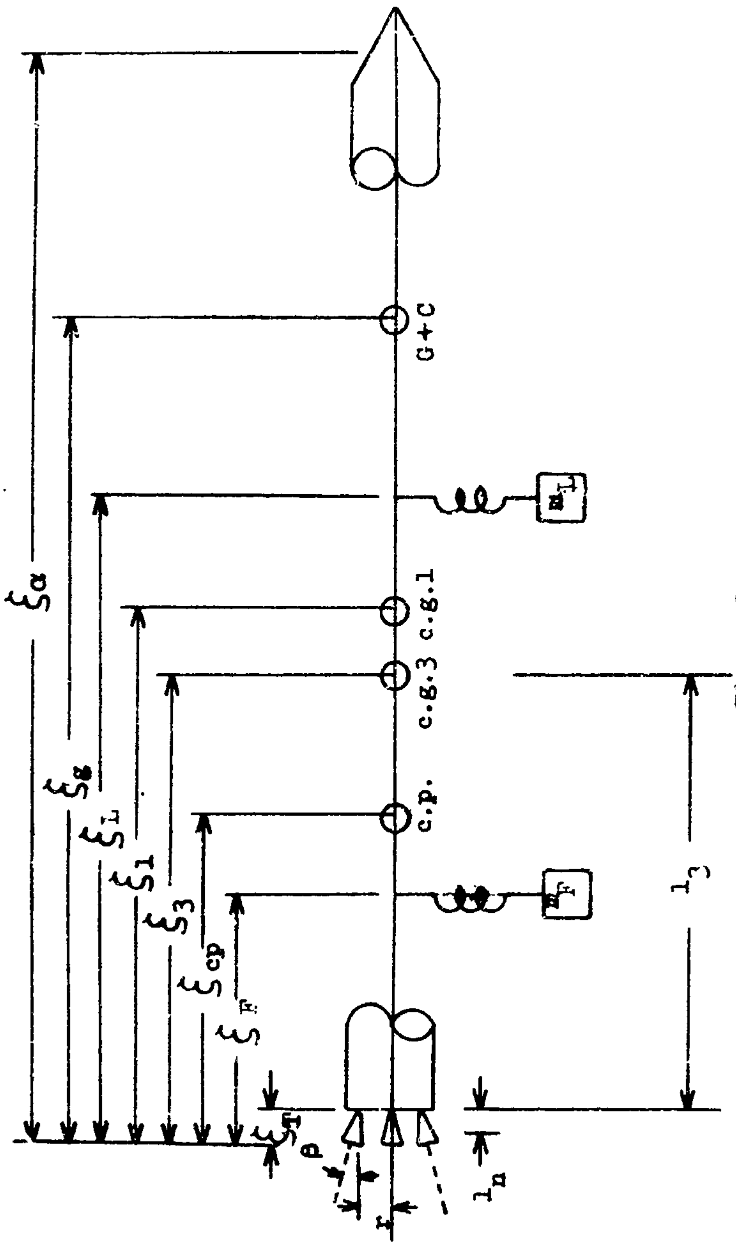

Figure 3

Missile Geometry for Angle-of-Attack Study

4. The effects of fluid sloshing in the tanks are neglected.

5. The effects of flexible body bending are neglected.

6. All sensor instrument dynamics are neglected.

4.1.1 Equations for Adaptive Angle-of-Attack System Digital Analysis

1. Moment Equation

$$s^2 \theta - \frac{N'(\xi_{cp} - \xi_1)}{I_1} \alpha + \left\{ \frac{I_n + m_n l_n l_1}{I_1} s^2 + \frac{\frac{T}{4}\left[l_1 + \sqrt{r^2 + l_1^2} \cos(\beta - \beta_{id}) + m_n l_n \frac{T-D}{M_1} \right]}{I_1} \right\} \delta = 0$$

2. Normal Force Equation

$$\left\{ (\xi_2 - \xi_1) s^2 - sV + g \cos \gamma_o \right\} \theta + \left\{ sV + \frac{T-D-M_1 g \cos \gamma_o + N'}{M_1} \right\} \alpha + \left\{ \frac{m_n l_n}{M_1} s^2 + \frac{R'}{M_1} \right\} \delta = 0$$

3. Engine Dynamics Equation

$$\frac{I_n + m_n l_n l_1}{I_n} s^2 \theta - \frac{m_n l_n N'}{I_n M_1} \alpha + \left\{ \left[1 - \frac{(m_n l_n)^2}{I_n M_1} \right] s^2 + 2 \zeta_n \omega_n s + \omega_n^2 + \frac{m_n l_n (T-D-R')}{I_n M_1} \right\} \delta + \left\{ -2 \zeta_n \omega_n s - \omega_n^2 \right\} \delta_a = 0$$

4. Angle-Of-Attack Meter Equation

$$\frac{\xi_\alpha - \xi_2}{V} s \theta - \alpha + \alpha_i = 0$$

5. Control Law Equation

$$\left\{ -a_1 s - a_o \right\} \theta - b_o \alpha_i + \delta_c^* = 0$$

6. Control Integrator Equation

$$\left\{ -s - K_I \right\} \delta_c^* + s \delta_c = 0$$

7. Actuator Equation

$$-\omega_a^2 \delta_c + \left\{ s^2 + 2 \zeta_a \omega_a s + \omega_a^2 \right\} \delta_a = 0$$

4.1.2 Table of Coefficients

		20 sec	67 sec	138.9 sec
$N'(\xi_{cp} - \xi_1)/I_1$	$1/sec^2$	.2215283	2.457713	.04534397
$\left\{ T/4 \left[l_1 + \sqrt{r^2 + l_1^2} \cos(\beta - \beta_{1d}) \right] + m_n l_n (T-D)/M_1 \right\} / I_1$	$1/sec^2$	1.505226	1.614720	3.760221
$(I_n + m_n l_n l_1)/I_1$	------	.00114589	.00112389	.00244245
$\xi_2 - \xi_1$	m	.0920378	.1217764	.4502196
V	m/sec	77	438	2410
$g \cos \gamma_o$	m/sec^2	9.782785	8.426664	5.042222
$(T - D - M_1 g \cos \gamma_o + N')/M_1$	m	5.40445	20.38[illegible]	51.[illegible]
$m_n l_n / M_1$	m	.004987937	.006903798	.01675426
R'/M_1	m/sec^2	7.3596861	11.200735	27.967829
$(I_n + m_n l_n l_1)/I_n$	-----	8.633642	8.256156	12.114934
$m_n l_n N'/I_n M_1$	$1/sec^2$	.3773256	5.7513439	.300600
$1 - (m_n l_n)^2 / I_n M_1$	-----	.996795	.995564	.989235
$2 \zeta_n \omega_n$	-----	8.7962	8.7962	8.7962
$\omega_n^2 + m_n l_n / I_n \left[(T-D-R')/M_1 \right]$	$1/sec^2$	3952.2621	3953.1353	3965.5573
ω_n^2	$1/sec^2$	3947.61	3947.61	3947.61
$(\xi_\alpha - \xi_2)/V$	sec	.405290415	.0725231141	.0105519004
$2 \zeta_a \omega_a$	1/sec	66.654	66.654	66.654
ω_a^2	$1/sec^2$	1190.25	1190.25	1190.25

4.2 Analog Computer Simulation

The equations, computer diagrams, and computed coefficients for use in the analog computer simulation of the missile dynamics for the study of the adaptive angle-of-attack control system are presented in this section. In using the equations in this section, an attempt is made to include all linear terms consistent with the following assumptions:

1. In writing the equations, all physical parameters of the missile such as mass, inertia, and thrust are considered constant. However, in performing the simulation, the significant time variable coefficients of the equations are varied. Some of the time variable coefficients of the equations which produce high frequency effects such as the engine reaction zero, or which do not vary significantly are held fixed at values corresponding to the time when maximum dynamic pressure occurs.

2. Aerodynamic forces are assumed to vary linearly with the total angle of attack developed by the centerline of the missile.

3. The dynamic equations are for motions in the missile yaw plane. The trim conditions on α, θ, and δ will be zero in this plane. The equations are also applicable to the pitch plane if the trimmed values of these variables may be neglected.

4. Fluid sloshing in the tanks is represented by two mass-spring analogs. One mass-spring analog is used to represent the fluid sloshing in the booster stage tanks and the other mass-spring analog is used to represent the fluid sloshing in the second stage tanks. The fluid slosh data given in Section 3.3 was reduced in the following manner: The fluid sloshing in the second stage LH_2 tank was neglected and only the fluid sloshing in the second stage LOX tank was included in the second stage slosh mode. The mass of the booster stage slosh mode is the sum of the sloshing masses in the booster stage tanks, the attach point is the center of mass of the sloshing masses in the booster stage tanks, and the frequency of booster stage slosh mode is the frequency of the large booster stage tank sloshing fluid. Nonlinear damping was added to the slosh modes to achieve marginal stability at the critical times of flight. The slosh data is used in this form since the slosh stability problem is not being considered in this study, and since the slosh modes are being included in the study to determine their effects on the adaptive angle-of-attack control system. This method of representing the slosh modes was adopted at the suggestion of Mr. Helmut Bauer of MSFC. It should be noted that the values of the sloshing masses

and the ratio of the two slosh mode frequencies are held fixed at the liftoff values.

5. The effects of flexible body bending are neglected.

6. All sensor instrument dynamics are neglected except for the accelerometer dynamics.

The computed coefficients for an all-engines-burning trajectory are presented in this section. This includes a table of the coefficients which remain constant with time, a table of the coefficients which are varied with time, and a table of the time variable coefficients which are held fixed at the values corresponding to when maximum dynamic pressure occurs.

4.2.1 Equations

1. Moment

$$I_3 \ddot{\theta} = -\left[\frac{T}{4}\left(l_3 + \sqrt{r^2 + l_3^2}\cos(\beta - \beta_{id})\right) + m_n l_n \frac{T - D}{M_1}\right]\delta$$

$$- \left[I_n + m_n l_n l_3\right]\ddot{\delta}$$

$$+ N'(\xi_{cp} - \xi_3)\alpha$$

$$+ m_L\left[\frac{T - D}{M_1} + \omega_L^2(\xi_L - \xi_3)\right]\lambda_L$$

$$+ m_F\left[\frac{T - D}{M_1} + \omega_F^2(\xi_F - \xi_3)\right]\lambda_F$$

$$- \frac{T}{8}\sqrt{r^2 + l_3^2}\,(\beta - \beta_{id})\ ^{*}$$

2. Acceleration Normal to Missile Centerline **

$$M_3 \ddot{Z}_{B_3} = R'\delta + m_n l_n \ddot{\delta} + N'\alpha$$

$$+ m_L\omega_L^2\lambda_L + m_F\omega_F^2\lambda_F + \frac{T}{8}\sin\beta\ ^{*}$$

3. Acceleration Normal to Reference **

$$\ddot{Z}_{T_g} = \ddot{Z}_{B_3} + (\xi_g - \xi_3)\ddot{\theta} + \frac{T - D}{M_1}\theta$$

4. Angular Relation

$$\alpha - \alpha_w = \psi$$

5. Normal Force Equation

$$V(\dot{\theta} - \dot{\psi}) = \ddot{Z}_{B_3} + (\xi_{\ } - \xi_3)\ddot{\theta}$$

$$+ g\cos\gamma_o(\theta - \psi) + \frac{T - D}{M_1}\psi$$

---

* Present only in engine-out case

** All $\ddot{Z}$ accelerations do not include gravity

6. Slosh Equations

$$\ddot{\lambda}_L = -\ddot{Z}_{B_3} - (\xi_L - \xi_3)\,\ddot{\theta} - 2\zeta_L\omega_L\dot{\lambda}_L - \omega_L^2\lambda_L$$

$$\ddot{\lambda}_F = -\ddot{Z}_{B_3} - (\xi_F - \xi_3)\,\ddot{\theta} - 2\zeta_F\omega_F\dot{\lambda}_F - \omega_F^2\lambda_F$$

7. **Engine Dynamics**

$$\ddot{\delta} = -\frac{I_n + m_n l_n l_3}{I_n}\,\ddot{\theta} + \frac{m_n l_n}{I_n}\,\ddot{Z}_{B_3}$$

$$+ 2\zeta_n\,\omega_n\,\dot{\delta}_a + \omega_n^2\,\delta_a$$

$$- 2\zeta_n\,\omega_n\,\dot{\delta} - \left(\omega_n^2 + \frac{m_n l_n}{I_n}\;\frac{T - D}{M_1}\right)\delta$$

8. **Actuator Equation**

$$\ddot{\delta}_a = \omega_a^2\,\delta_c - 2\zeta_a\,\omega_a\,\dot{\delta}_a - \omega_a^2\,\delta_a$$

9. **Angle-of-Attack Meter Equation**

$$\alpha_i = -\frac{\xi_\alpha - \xi_2}{V}\,\dot{\theta} + \alpha$$

10. **Accelerometer Dynamics**

$$\ddot{A}_i = \omega_A^2\,\ddot{Z}_{B_3} + \omega_A^2\,(\xi_A - \xi_3)\,\ddot{\theta}$$

$$- 2\zeta_A\,\omega_A\,\dot{A}_i - \omega_A^2\,A_i$$

11. **Measured Acceleration Normal to Reference**

$$\ddot{Z}_{T_i} = A_i + \frac{T - D}{M_1}\,\theta$$

4.2.2 Analog Computer Mechanization

This section contains diagrams of the analog computer setup used in the study of the programmed and the adaptive angle-of-attack control systems. A discussion of the check procedure used to verify the analog computer mechanization is also included.

Figures 4 and 5 are the mechanization diagrams of the missile dynamics as described by the equations listed in Section 4.2.1. Figures 6 and 7 are the mechanization diagrams for the wind disturbances and the engine out disturbance. In this study, the engine out disturbance consisted of the inclusion of a disturbance moment and a disturbance normal force and the reduction of the control moment per unit of control deflection. The engine failure was simulated by using an exponential thrust decay with a one-third second time constant.

A detailed check procedure was used to verify the analog computer mechanization of the missile dynamics and the basic angle-of-attack control system. Frequency response checks of the analog computer mechanization were made at two times of flight with all time-varying coefficients fixed. These results were compared with the frequency response data obtained from the digital computer analysis of the simplified system equations given in Section 4.1.1, and the results agreed. Transient responses to step changes in angle of attack due to wind and to step attitude position commands were also measured at two times of flight and compared with the results of digital computer solutions of the simplified equations. These results also agreed. Finally, static checks of the analog computer mechanization were made, and all time-variable coefficients were checked by reading them out on an x-y plotter.

Definition of Variable Parameters on Computer Mechanization Diagrams

$$f_n = d_n\,(x_n + e_n/d_n)$$

n	f_n
1	$\frac{T}{4}\left[l_3 + \sqrt{r^2 + l_3^2}\,\cos\,(\beta - \beta_{id})\right] + m_n\, l_n\,(T - D)/M_1$
2	$N'(\xi_{cp} - \xi_3)$
3	$1/I_3$
4	$M_L\left[(T - D)/M_1 + \omega_L^2(\xi_L - \xi_3)\right]$
5	$M_F\left[(T - D)/M_1 + \omega_F^2(\xi_F - \xi_3)\right]$
6	$T/8\,\sqrt{r^2 + l_3^2}\,(\beta - \beta_{id})$
7	R'
8	N'
9	$1/M_3$
10	$(T - D)/M_1$
11	$(T - D)/M_3$
12	$1/V$
13	$g\cos\gamma_o/V$
14	ω_F^2
15	$\xi_L - \xi_3$
16	$\xi_F - \xi_3$
17	$(\xi_\alpha - \xi_2)/V$
18	q
19	k

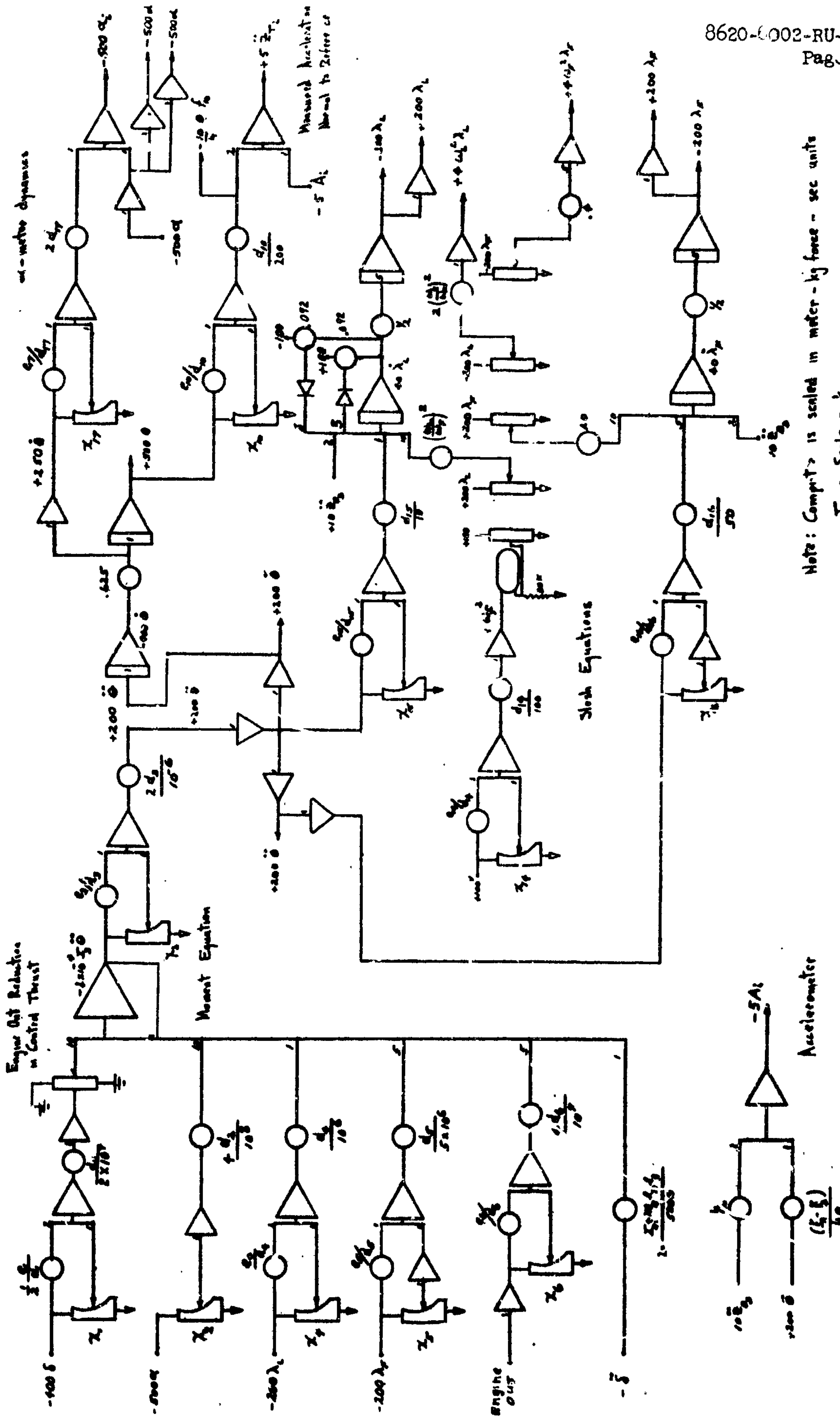

Figure 4

Missile Dynamics Computer Mechanization - Sheet 1

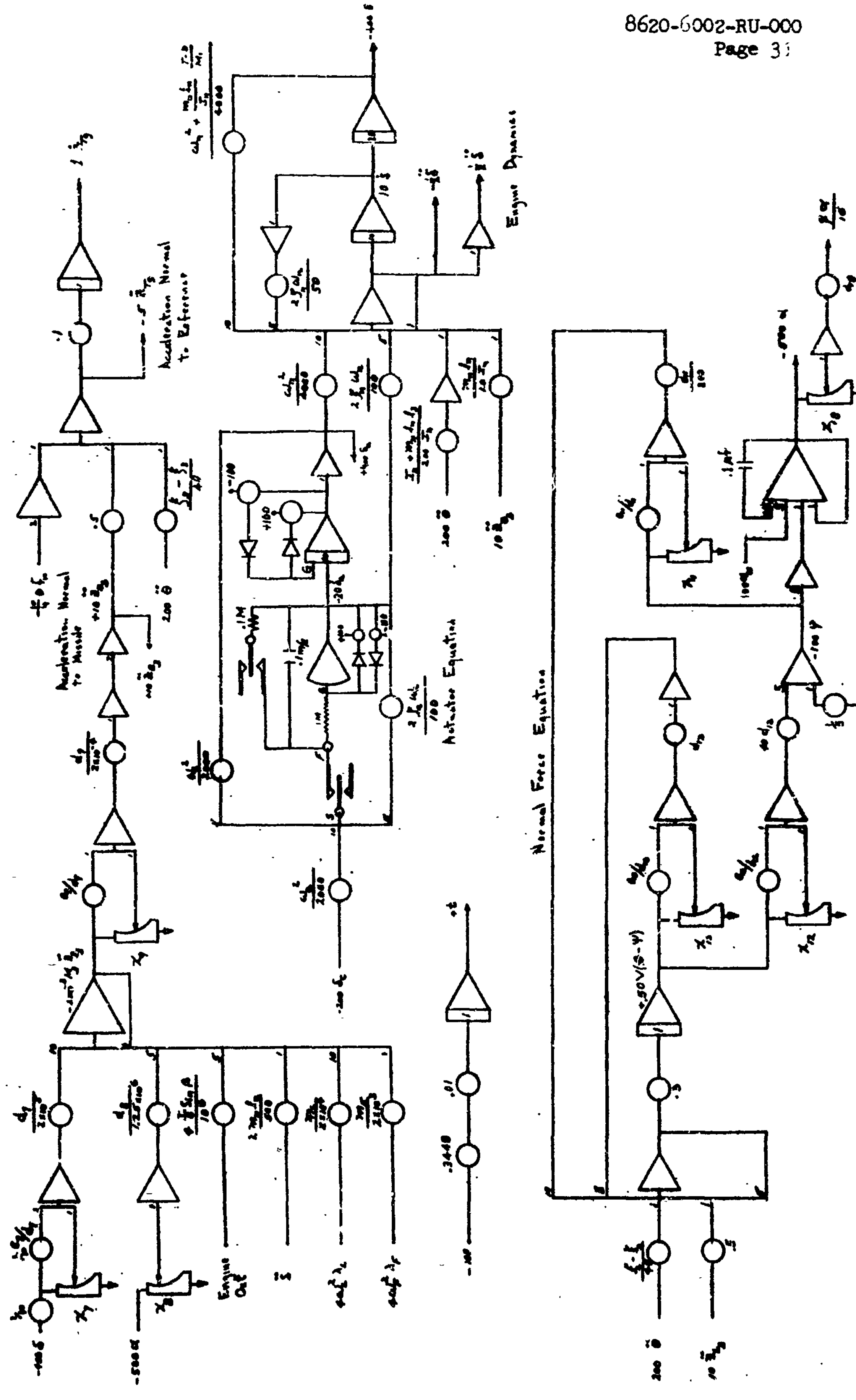

Figure 5
Missile Dynamics Computer Mechanization - Sheet 2

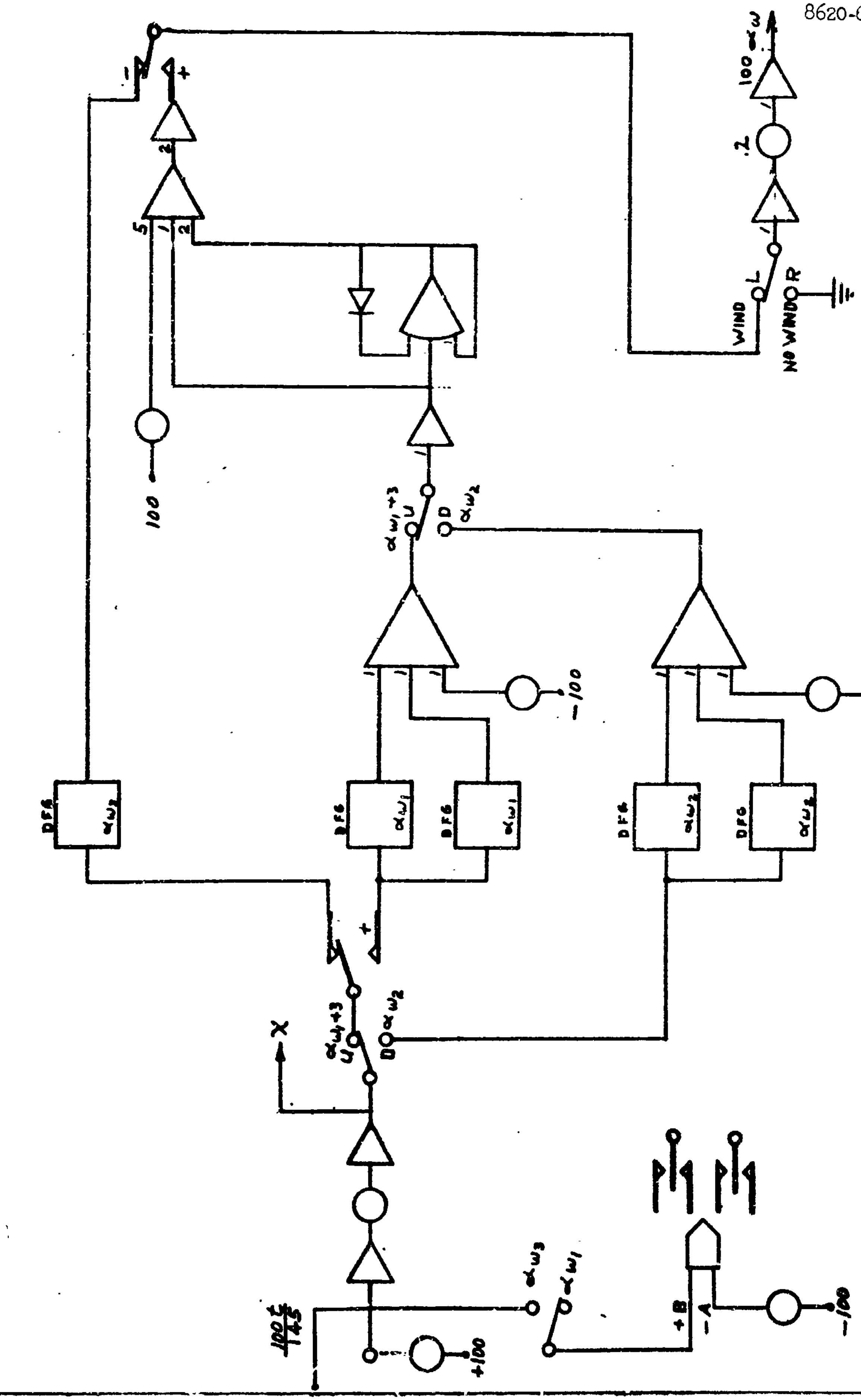

Figure 6
Wind Disturbance Computer Mechanization

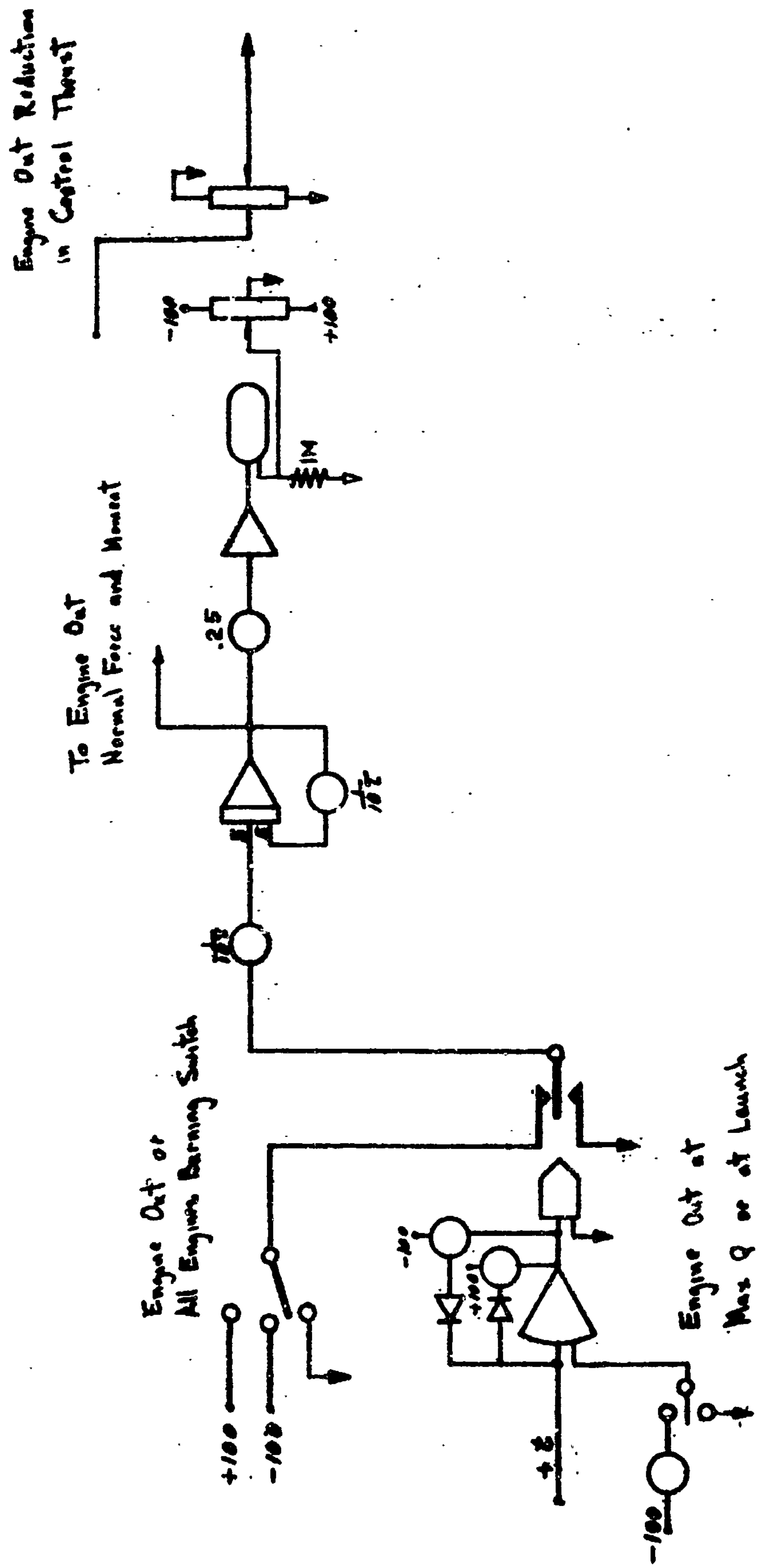

Figure 7

Engine Out Disturbance Computer Mechanization

4.2.3 **Table of Constant Coefficients**

m_L	2647.2183	kg-sec^2/m
m_F	1156.1508	kg-sec^2/m
$m_n l_n$	204.67	kg-sec^2/m
$m_n l_n / I_n$	.64253	m^{-1}
ω_L/ω_F	.5883045	
$(\omega_L/\omega_F)^2$	.3461022	
$\omega_A^{\;2}$	3197.90	sec^{-2}
$2\zeta_A\omega_A$	79.[illegible]70	sec^{-1}
$\omega_a^{\;2}$	1190.25	sec^{-2}
$2\zeta_a\omega_a$	66.654	sec^{-1}
$\omega_n^{\;2}$	3947.61	sec^{-2}
$2\zeta_n\omega_n$	8.7962	sec^{-1}

4.2.4 Table of Variable Coefficients

Time	$\frac{T}{4}\left[l_3+\sqrt{r^2+l_3^2}\cos(\beta-\beta_{1d})+m_n l_n \frac{T-D}{M_1}\right]$	$N'(\xi_{cp}-\xi_3)$	$1/I_3$	$m_L\left[\frac{T-D}{M_1}+\omega_L^2(\xi_L-\xi_3)\right]$	$m_F\left[\frac{T-D}{M_1}+\omega_F^2(\xi_F-\xi_3)\right]$	$\frac{T}{8}\sqrt{r^2+l_3^2}(\beta-\beta_{1d})$	R'
Sec	kg m	kg m	$kg^{-1} sec^{-2} m^{-1}$	kg	kg	kg m	kg
0	3524027	.0	$.43683X10^{-6}$	203707	120374	-87834	278345
10	3444800	123703	$.45000X10^{-6}$	212542	105087	-90490	299265
20	3408227	548547	$.46132X10^{-6}$	227409	90427.9	-93126	301990
30	3368470	1406703	$.47001X10^{-6}$	246182	76770.[illegible]	-97053	306715
40	3387380	2722277	$.47551X10^{-6}$	271028	58965.6	-100454	313125
50	3436178	4301917	$.47619X10^{-6}$	294794	34997.4	-103636	320500
60	3479823	5430740	$.47735X10^{-6}$	322484	6126.67	-106872	327700
67	3493467	5985020	$.48102X10^{-6}$	352191	-15858.2	-109146	332057
70	3531857	5860357	$.48288X10^{-6}$	361809	-29832.3	-109104	333660
80	3611764	5314258	$.48527X10^{-6}$	402028	-79825.5	-109437	337645
90	3724638	4183203	$.48943X10^{-6}$	440624	-148262	-107826	339905
100	3652598	2585712	$.49407X10^{-6}$	485100	-239817	-105114	340995
110	4141259	1255974	$.50695X10^{-6}$	510964	-383190	-97766	341430
120	4611167	525921.7	$.54693X10^{-6}$	508663	-602972	-85447	341585
130	5370487	195906.5	$.63099X10^{-6}$	449728	-953616	-65662	341635
138.9	6293281	65859.8	$.78697X10^{-6}$	324441	-1422018	-41491	341655
144.9	3378434	23724.9	$.91642X10^{-6}$	165623	-1820959	-14682	170830

Time	N'	$1/M_3$	$\frac{T-D}{M_1}$	$1/V$	$g \cos \gamma_0 / V$	ω_F^2	$\xi_L - \xi_3$
Sec	kg	m/kg sec^2	m/sec^2	sec/m	sec^{-1}	sec^{-2}	m
0	.000000	$.23766 \times 10^{-4}$	13.0	∞	∞	20.430	9.0383
10	5488.6736	$.25258 \times 10^{-4}$	13.7	.0277778	.2719447	20.612	9.3407
20	24096.62	$.26860 \times 10^{-4}$	14.6	.0129870	.1270490	21.530	9.5674
30	60977.8	$.28730 \times 10^{-4}$	15.6	.00757576	.0736752	22.658	9.8720
40	117496	$.30879 \times 10^{-4}$	16.8	.00505051	.0482537	24.602	10.0373
50	185942	$.33377 \times 10^{-4}$	17.7	.00361011	.0333567	26.729	10.1346
60	237025	$.36312 \times 10^{-4}$	18.3	.00273973	.0241074	29.268	10.2373
67	265364	$.38695 \times 10^{-4}$	19.8	.00228311	.019239	31.655	10.3361
70	264410	$.39815 \times 10^{-4}$	20.7	.00211416	.0174368	32.604	10.2724
80	255325	$.44066 \times 10^{-4}$	23.8	.00162338	.0124206	36.361	10.1625
90	216597	$.49334 \times 10^{-4}$	27.2	.00125313	.00885465	40.577	9.9024
100	143689	$.56029 \times 10^{-4}$	31.0	.00097943	.00639112	45.968	9.5634
110	75768.8	$.64830 \times 10^{-4}$	35.3	.00077519	.00469317	52.148	8.7321
120	34607.4	$.76911 \times 10^{-4}$	40.6	.00062112	.00355699	59.598	7.3525
130	14864.6	$.74527 \times 10^{-4}$	47.5	.00050125	.00265829	68.890	5.1393
138.9	5716.25	$.11886 \times 10^{-3}$	55.9	.00041494	.00209222	79.032	2.4370
144.9	2233.957	$.13011 \times 10^{-3}$	29.7	.00039170	.00191737	87.984	1.0786

Time	$\xi_F - \xi_3$	$(\xi_\alpha - \xi_2)/V$	q	k	α_{w_1}	α_{w_2}	α_{w_3}
Sec	m	sec	kg/m^2	--	rad	rad	rad
0	4.4599	∞	.0000	.0000	.0000	∞	.0000
10	3.7451	.88004	82	.0249551	.0122	.1569	.0122
20	2.9547	.41434	360	.10210951	.0201	.0945	.0201
30	2.2421	.24397	911	.2253401	.0302	.0822	.0302
40	1.3902	.16345	1738	.3590388	.0380	.0811	.0380
50	.4703	.11716	2684	.4746942	.0455	.0849	.0455
60	-.4442	.089170	3325	.5447128	.0630	.0903	.0630
67	-1.0574	.074518	3524	.5652331	.1712	.1712	.1712
70	-1.4263	.068860	3435	.550270	.0803	.0803	.1586
80	-2.5534	.052670	[illegible]	5202750	.0201	.0433	.0866
90	-3.8307	.040304	2143	.4534933	.0008	.0157	.0313
100	-5.1868	.031140	1274	.3358121	.0000	.0122	.0245
110	-7.0353	.023964	545	.1957609	.0000	.0180	.0360
120	-9.4321	.018295	298	.09234329	.0000	.0246	.0492
130	-12.6625	.013583	135	.03776718	.0000	.0295	.0590
138.9	-16.270	.010030	61	.01381375	.0000	.0290	.0581
144.9	-18.2388	.0088872	25	.01067730	.0000	.0274	.0548

4.2.5 Table of Variable Coefficients Which Are Held Fixed

Time	$\frac{T}{g}\sin\beta$	$I_n+m_n l_n l_3$	$(I_n+m_n l_n l_3)/I_n$	$\xi_2-\xi_3$	$\xi_g-\xi_3$	$\omega_n^2+\frac{m_n l_n}{I_n}\times\frac{T-D}{M_1}$	$\omega_A^2(\xi_A-\xi_3)$
Sec	kg	kg sec^2 m	-----	m	m	sec^{-2}	m/sec^2
0	7796.352	2715.06	8.5234	.0885	27.1528	3955.96	86831.9
10	7820.393	2653.17	8.3291	.0918	27.4552	3956.41	87799.0
20	7891.603	2606.77	8.1834	.0959	27.6819	3956.99	88523.9
30	8015.076	2544.43	7.9877	.0999	27.9865	3957.63	89498.0
40	8182.583	2510.60	7.8815	.1059	28.1518	3958.40	90026.6
50	8375.306	2490.68	7.8190	.1136	28.2491	3958.98	90337.8
60	8563.456	2469.66	7.7530	.1226	28.3518	3959.37	90665.2
67	8677.300	2449.44	7.6895	.1296	28.4506	3960.33	90982.2
70	8719.203	2462.48	7.7305	.1342	28.3869	3960.91	90778.5
80	8823.339	2484.97	7.8011	.1501	28.2770	3962.90	90427.0
90	8882.397	2538.21	7.9682	.1723	28.0169	3965.09	89595.2
100	8910.881	2607.59	8.1860	.2017	27.6779	3967.53	88511.2
110	8922.249	2777.73	8.7201	.2505	26.8466	3970.29	85852.7
120	8926.299	3060.09	9.6065	.3306	25.4670	3973.70	81440.9
130	8927.606	3513.07	11.029	.4728	23.2538	3978.13	74363.3
138.9	8928.128	4066.15	12.765	.6984	20.5515	3983.53	65721.6
144.9	4464.130	4344.17	13.638	.8220	19.1931	3966.69	61377.6

5. ADAPTIVE DIGITAL-COMPENSATION STUDY

This section contains the equations and parameters for use in the study of flexible-body stability using an adaptive digital-compensation control system. The coordinate system and missile geometry conventions used are shown in Figures 8 and 9.

In using the equations listed in this section in 5.1, an attempt is made to include all linear terms consistent with the following assumptions:

1. All physical parameters of the missile such as mass, inertia, and thrust are considered constant.
2. Aerodynamic forces are assumed to be independent of the local bending slope and are assumed to vary linearly with the total angle of attack developed by the average centerline of the missile.
3. The dynamic equations are for motions in the missile yaw plane. The trim conditions on α, θ, and δ will be zero in this plane. The equations are also applicable to the pitch plane if the trimmed values of these variables may be neglected.
4. Normal modes are determined for free-free end conditions and include effects of bending and shear. Effect of axial force on bending is neglected. The bending mode data given in Section 3.4, which were generated with the control engines removed, have been renormalized to give bending modes for the complete missile with locked actuators and with modal masses equal to the total mass of the missile. The data was renormalized to this form to allow simplification of the equations and, thus, reduced complexity in the analog computer mechanization.
5. The control thrust, defined as the thrust available for control in a given plane, is equal to 1/2 the total thrust and comes from one engine on the missile body centerline.
6. The effects of fluid sloshing in the tanks are neglected.

The basic missile and trajectory parameters used in the linear stability studies of the Saturn C-1 configuration are given in Sections 5.2, 5.3, and 5.4. These parameters were used as inputs to the digital computer runs used in the linear stability studies. Section 5.2 lists the parameters that remain constant during the booster flight. Section 5.3 lists the variable parameters at the three times of flight which were investigated. Section 5.4 describes the renormalization computation made on the bending data given in Section 3.4. The renormalized bending data is presented in graphical form.

The analog computer mechanization of the missile dynamics used in this study is described in Section 5.5. The computed coefficients of the equations mechanized are listed in Section 5.6.

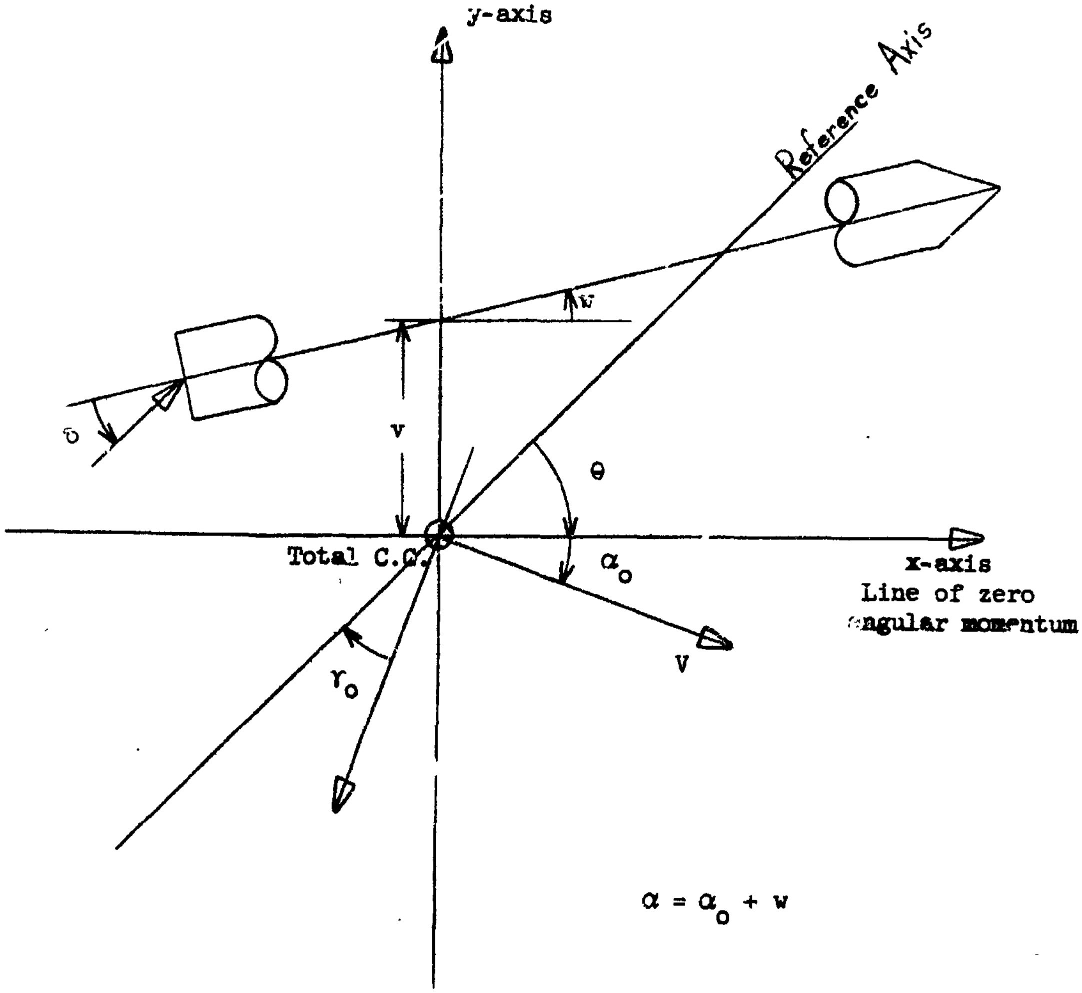

Figure 8
Coordinate System for Bending Study

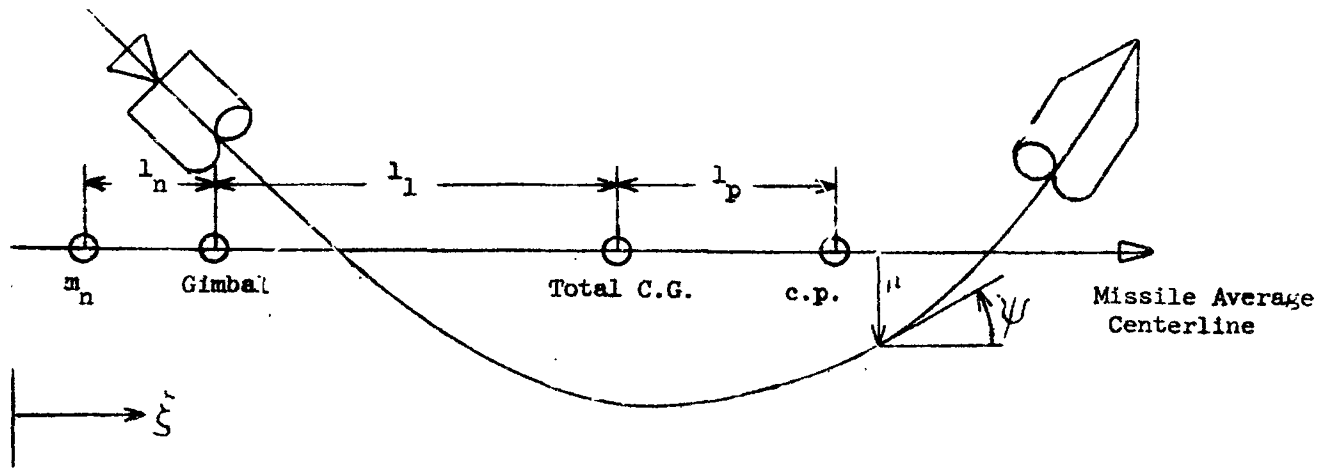

Figure 9

Missile Geometry for Bending Study

5.1 Equations

1. Acceleration Equations

$$M_1 a_y - N'\alpha + (M g \cos\gamma_o)\,\theta + Dw - T\,\psi_T - R'\delta + \frac{T}{8}\sin\beta^* = 0$$

$$a_x = \frac{T-D}{M} - g\cos\gamma_o$$

2. Normal Force Equation

$$a_y + (Vs + a_x)\alpha + Vs\theta - (Vs + a_y)w + (Vs + a_x)\alpha_w = 0$$

3. Moment Equation

$$\frac{N'l_p}{I_1}\alpha + s^2\theta + \frac{D}{I_1}\,v - \frac{T}{I_1}\,\mu_T + \frac{T}{8\,I_1}\left[r^2 + l_1{}^2\right]^{\frac{1}{2}}(\beta - \beta_{id})^*$$

$$- \frac{Tl_1}{I_1}\,\psi_T - \frac{R'l_1}{I_1}\,\delta = 0$$

4. Centerline Deflection Equation

$$M_1 v - m_n l_n \delta = 0$$

5. Centerline Rotation Equation

$$I_1 w + (I_n + l_1 l_n m_n)\delta = 0$$

6. Gimbal Displacement Equation

$$\mu_T - v + l_1\,w - \sum_i \phi_i(\xi_T)\,q_i = 0$$

7. Gimbal Slope Equation

$$\psi_T - w - \sum_i \phi_i{}'(\xi_T)\,q_i = 0$$

8. Bending Mode Amplitude Equation

$$\frac{T-D}{M_1}\phi_i{}'(\xi_T)\,v - \frac{T}{M_1}\,\phi_i(\xi_T)\,\psi_T + \frac{T}{8\,M_1}\sin\beta\,\phi_i(\xi_T)^*$$

$$- \frac{T}{8\,M}\,r\cos\beta\,\phi_i{}'(\xi_T)^* + (s^2 + 2\zeta_i\,\omega_i\,s + \omega^2{}_i)\,q_i$$

$$+ \left[\frac{I_n}{M_1}\,\phi_i{}'(\xi_T)\,s^2 - \frac{m_n l_n}{M_1}\,\phi_i(\xi_T)\,s^2 - \frac{R'}{M_1}\phi_i(\xi_T)\right]\delta = 0$$

* Present only in engine out case.

9. Engine Dynamics Equation

$$- \frac{m_n l_n}{I_n} a_y - \left[\frac{I_n + l_1 l_n m_n}{l_n} s^2 + \frac{m_n l_n}{I_n} g \cos \gamma_o \right] \theta$$

$$+ \frac{T-D}{I_n} v - \frac{m_n l_n}{I_n} s^2 \mu_T + \left[s^2 + \frac{m_n l_n}{M_1 I_n} (T-D) \right] \psi_T$$

$$+ s^2 \delta + \left[2 \zeta_n \omega_n s + \omega^2_n \right] (\delta - \delta_a) = 0$$

10. Attitude Rate Sensor Equation

$$\frac{1}{\omega^2_R} \left[s^2 + 2 \zeta_R \omega_R s + \omega^2_R \right] \dot{\theta}_R = s \left[\theta - w - \sum_i \theta'_i (\xi_R) q_i \right] \left[\frac{1}{\tau_P s + 1} \right]$$

11. Attitude Position Sensor Equation

$$\left[\tau_P s + 1 \right] \theta_P = \theta - w - \sum_i \phi'_i (\xi_P) q_i$$

12. Hydraulic System Equation

$$(s^2 + 2 \zeta_a \omega_a s + \omega^2_a) \delta_a = \omega^2_a \delta_c$$

13. Lateral Acceleration Sensor Equation

$$a_n + a_y - (l_A s^2 + a_x) \theta + s^2 v + l_A s^2 w$$

$$+ \sum_i \phi_i (\xi_A) s^2 q_i = 0$$

5.2 Table of Constant Parameters

$1/2\ m_n$	100.24	slugs
l_n	2.25	ft
$1/2\ I_n$	1152	slug-ft^2
ω_n	62.8	rad/sec
ζ_n	0.07	
$2\ \zeta_n \omega_n\ (1/2\ I_n)$	10128	ft-lb-sec
$2\ \zeta_n \omega_n$	8.792	1/sec
$\omega_a^{\ 2}$	1190.5	1/sec^2
$2\ \zeta_a\ \omega_a$	66.67	1/sec
ω_R	188.4	rad/sec
ζ_R	0.7	
τ_P	$\frac{1}{282.6}$	sec
A	360.24	ft^2
g	32.12	ft/sec^2
ξ_T	100	in
ξ_R	750	in
ξ_P	1630	in
ξ_A	1800	in

5.3 Table of Variable Parameters

		Liftoff (t=0)	Max Q (t=67)	Burnout (t=138.9)
M	slugs	30829	19921	8209
I	slug-ft^2	18.1×10^6	16.9×10^6	11.4×10^6
γ_o	rad		.534071	1.029745
V	ft/sec	0	1437	7907
T	lb	1315476	1464118	1506440
q	lb/ft^2	0	721.8	12.5
C_{N_α}	rad^{-1}	2.00	2.25	2.80
D	lb	0	172710	461
ξ_1	in	585.73	547.18	783.62
ξ_{cp}	in	1436.4	1397.85	1274.49
ω_1	rad/sec	10.20174	13.12642	16.14596
ω_2	rad/sec	28.46236	31.22392	45.52398
ω_3	rad/sec	43.32002	49.88555	85.67030
ζ_1		0.005	0.005	0.005
ζ_2		0.005	0.005	0.005
ζ_3		0.005	0.005	0.005

5.4 Renormalized Bending Data

The renormalized bending data, used in the linear stability studies described in Volume 1 and in the simulation of the missile dynamics for the study of the adaptive system, are presented in this section. This data is different from the bending mode data provided by MSFC for this study, which was generated with the control engines removed and is presented in Section 3.4. The original data was renormalized to give bending modes for the complete missile with locked actuators and with modal masses equal to the total mass of the missile. The method of renormalization used is described in detail in this section. The procedure was used to allow simplification of the missile dynamic equations by decoupling the bending modes and, thus, to reduce the complexity in the analog computer mechanization of these equations.

Plots of the modal deflections and slopes for the first three renormalized bending modes are presented in Figures 10 to 15.

With no external forces, such as aerodynamic forces, gravity, or thrust, acting on the missile, with actuators locked, using bending data generated with control engines removed, and neglecting structural damping, the missile dynamic equations reduce to:

$$A_i \ddot{v} + B_i \ddot{w} + \sum_{j=1}^{3} C_{ij} \ddot{Q}_j + M_B \Omega_i^2 Q_i = 0 \quad (i=1,2,3) \tag{5.4.1}$$

$$M v + \sum_{j=1}^{3} A_j Q_j = 0 \tag{5.4.2}$$

$$I w + \sum_{j=1}^{3} B_j Q_j = 0 \tag{5.4.3}$$

where

$$A_i = m_n \varphi_i (\zeta_T) - l_n m_n \varphi_i' (\zeta_T)$$

$$B_i = -l_1 A_i - m_n l_i$$

$$C_{ij} = \varphi_i(\hat{\xi}_T)\,\dot{A}_j - m_n\, l_j\, \varphi_i'(\hat{\xi}_T) + \begin{cases} M_B & i=j \\ 0 & i \neq j \end{cases}$$

$$l_i = l_n\, \varphi_i(\hat{\xi}_T) - \frac{I_n}{m_n}\, \varphi_i'(\hat{\xi}_T)$$

$$M_B = M - m_n$$

Substituting Equations 5.4.2 and 5.4.3 into Equation 5.4.1 and writing this result in matrix form gives

$$[M]\,[Q]\, s^2 + [K]\,[Q] = 0 \tag{5.4.4}$$

With the equations written in this form, the coupling between the modes due to the engine results in off-diagonal terms in the matrix $[M]$. This matrix can be diagonalized, which decouples the bending modes, by expanding the coupled amplitude functions, Q_i, as a series of orthogonal functions, q_i, such that

$$Q_j = \sum_i e_{ji}\, q_i \tag{5.4.5}$$

or, in matrix notation

$$[Q] = [E]\,[q] \quad . \tag{5.4.6}$$

The $[E]$ matrix is the modal matrix determined by solution of the characteristic value problem

$$[M]\,[E]\,[\omega^2] = [K]\,[E] \tag{5.4.7}$$

where $[\omega^2]$ is a diagonal matrix with diagonal elements equal to the squares of the uncoupled frequencies (eigenvalues of the characteristic value problem).

Solution of the characteristic value problem, Equation 5.4.7, makes it possible to write the bending equations, Equation 5.4.4, in the form

$$M \left\{ s^2\, [I]\,[q] + [\omega^2]\,[q] \right\} = 0 \tag{5.4.8}$$

where $\left[I\right]$ is the identity matrix.

The modal matrix, $\left[E\right]$, has been normalized with respect to the total mass such that

$$\left[E\right]_T \left[M\right] \left[E\right] = M \left[I\right] \qquad (5.4.9)$$

where $\left[E\right]_T$ represents the transposed modal matrix.

The displacement of the missile centerline may be expressed as follows:

$$u = \sum_j \phi_j q_j = \sum_j \varphi_j Q_j + v + xw \qquad (5.4.10)$$

where ϕ_j is the mode deflection corresponding to the orthorgonal modal amplitude function, q_j, and $x = \frac{1}{12} (\xi - \xi_1)$.

Substituting Equations 5.4.2 and 5.4.3 into 5.4.10, this becomes

$$\sum_j \phi_j q_j = \sum_j (\varphi_j - \frac{A_j}{M} - x \frac{B_j}{I}) Q_j \qquad (5.4.11)$$

or in matrix notation

$$\left[\phi\right]_T \left\{q\right\} = \left[\varphi - \frac{A}{M} - x \frac{B}{I}\right]_T \left\{Q\right\} \qquad (5.4.12)$$

Substituting Equation 5.4.6 into 5.4.12,

$$\left[\phi\right]_T \left\{q\right\} = \left[\varphi - \frac{A}{M} - x \frac{B}{I}\right]_T \left[E\right] \left\{q\right\} \qquad (5.4.13)$$

Thus,

$$\left[\phi\right]_T = \left[\varphi - \frac{A}{M} - x \frac{B}{I}\right]_T \left[E\right] \qquad (5.4.14)$$

or

$$\phi_i = \sum_j (\varphi_j - \frac{A_j}{M} - x \frac{B_j}{I}) e_{ji} \qquad (5.4.15)$$

The rotation of the missile centerline and center of mass may be expressed as follows:

$$\Psi = \sum_j \phi'_j q_j = \sum_j \varphi'_j Q_j + w \qquad (5.4.16)$$

where ϕ'_j is the mode slope corresponding to the orthogonal modal amplitude function, q_j.

Following the same procedure as above, the following is obtained:

$$\phi'_j = \sum_j \left(\varphi'_j - \frac{B_j}{I} \right) e_{ji} \qquad (5.4.17)$$

Thus, Equations 5.4.15 and 5.4.17 and the modal matrix $\left[E\right]$ are used to obtain the renormalized mode deflections and slopes. The diagonal matrix $\left[\omega^2\right]$ has as diagonal elements, the squares of the renormalized mode frequencies.

The original bending data, which was normalized to have unity deflection at the nose, was first renormalized, so that the modal mass of each mode equaled the total mass of the missile, by multiplying the mode data by $\sqrt{M/m_i}$. Thus,

$$\varphi_i = \left[M/m_i \right]^{\frac{1}{2}} \bar{\varphi}_i \qquad (5.4.18)$$

and

$$\varphi'_i = \left[\frac{M}{m_i} \right]^{\frac{1}{2}} \bar{\varphi}'_i \qquad (5.4.19)$$

where $\bar{\varphi}_i$ and $\bar{\varphi}'_i$ are the mode deflections and slopes of the original bending data.

A generalized eigenvalue digital computer program was then used to solve for the eigenvalues and eigenvectors of Equation 5.4.4. The eigenvalues obtained were then the renormalized mode frequencies, ω_i. The eigenvectors obtained were normalized by assuming

$$\left[E\right]_T \left[M\right] \left[E\right] \approx M \left[E\right]_T \left[E\right] \qquad (5.4.20)$$

Thus, by Equation 5.4.9

$$\left[E\right]_T \left[E\right] \approx \left[I\right] \qquad (5.4.21)$$

or

$$\sum_j e_{ji}^2 = 1 \qquad (i=1,2,3) \qquad (5.4.22)$$

The modal matrix $\left[E \right]$, and Equations 5.4.15 and 5.4.17 were used to compute the renormalized mode deflections and slopes. The results are plotted in Figures 10 to 15. The renormalized mode frequencies are given in Section 5.3.

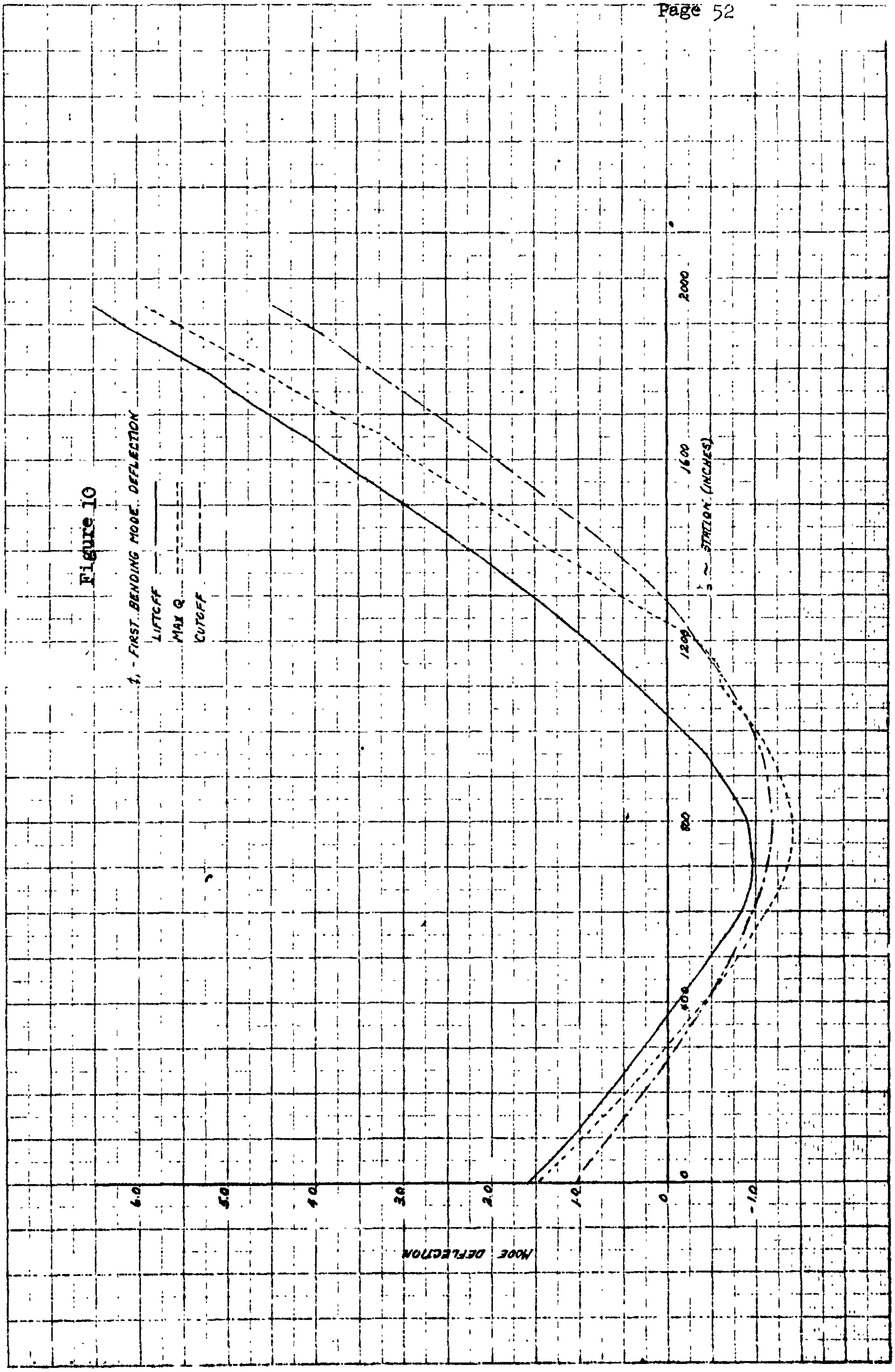
1. - FIRST BENDING MODE DEFLECTION
LIFTOFF
MAX Q
CUTOFF
MODE DEFLECTION
6.0
5.0
4.0
3.0
2.0
1.0
0
-1.0
0
400
800
1200
1600
2000
STATION (INCHES)

Figure 10

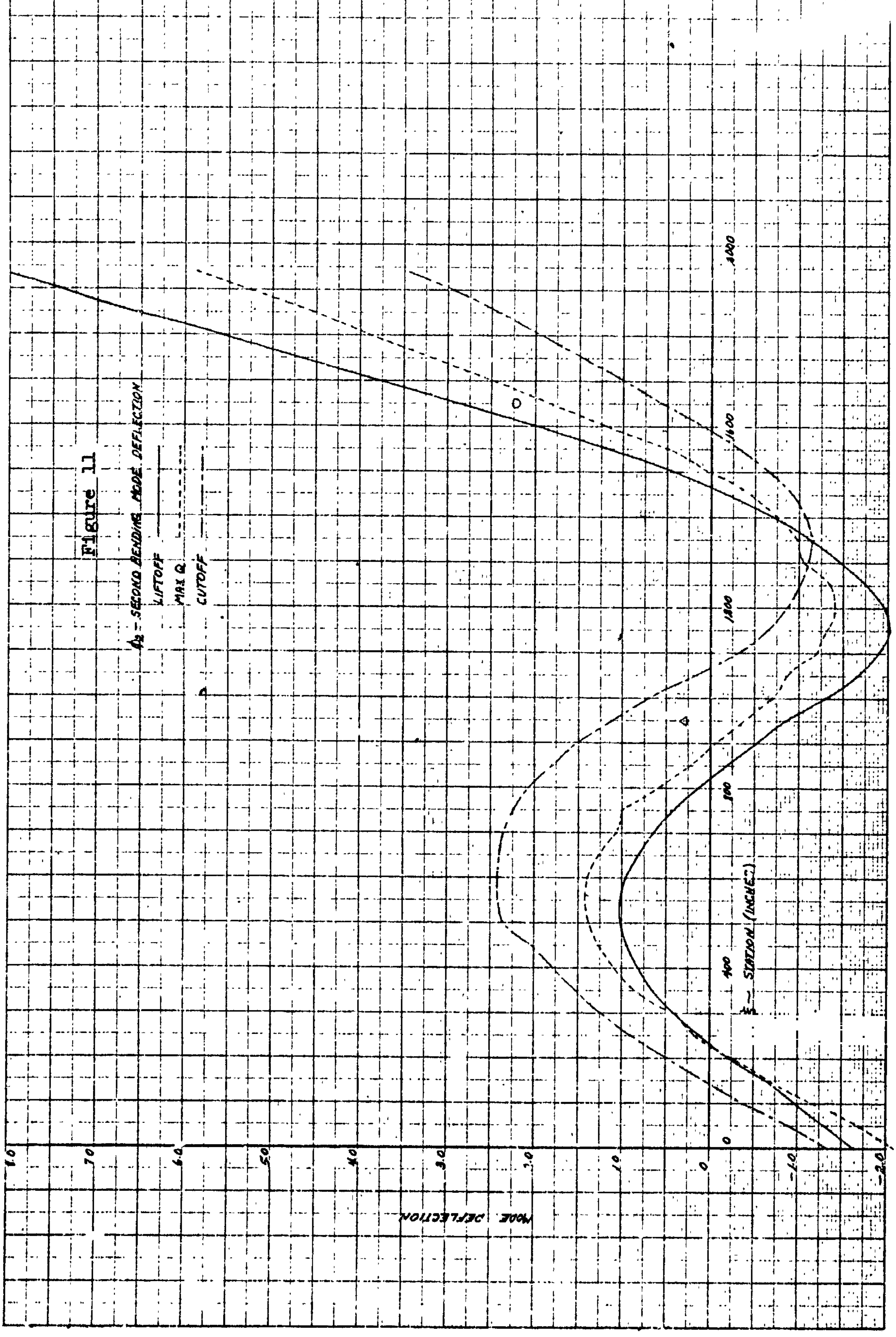
Φ_2 - SECOND BENDING MODE DEFLECTION
LIFTOFF
MAX Q
CUTOFF
STATION (INCHES)
MODE DEFLECTION
0
400
800
1200
1600
2000

Figure 11

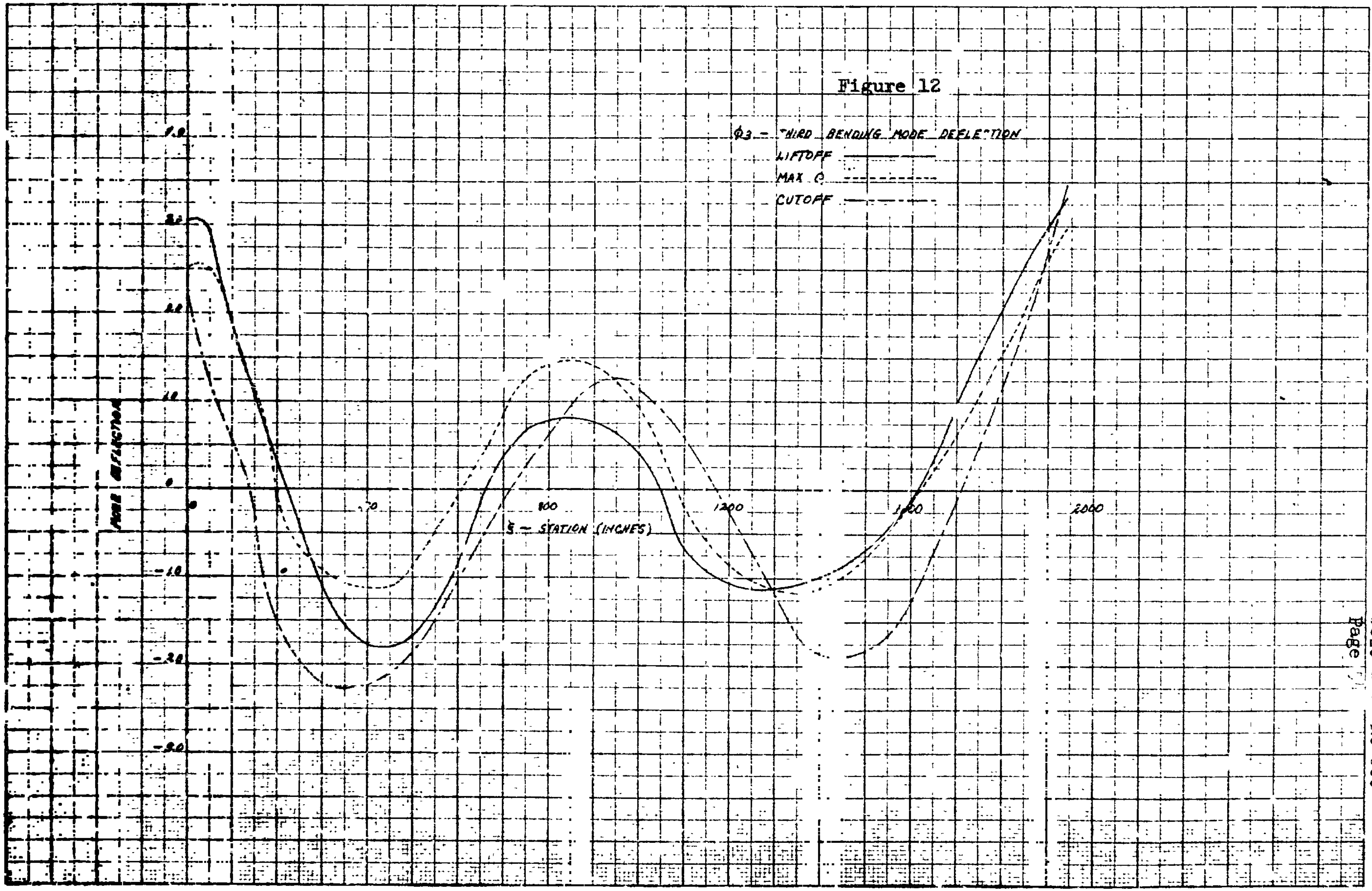
φ3 — THIRD BENDING MODE DEFLECTION
LIFTOFF
MAX Q
CUTOFF
MODE DEFLECTION
ξ — STATION (INCHES)
0
800
1200
2000
-1.0
-2.0
-3.0

Figure 12

Figure 13

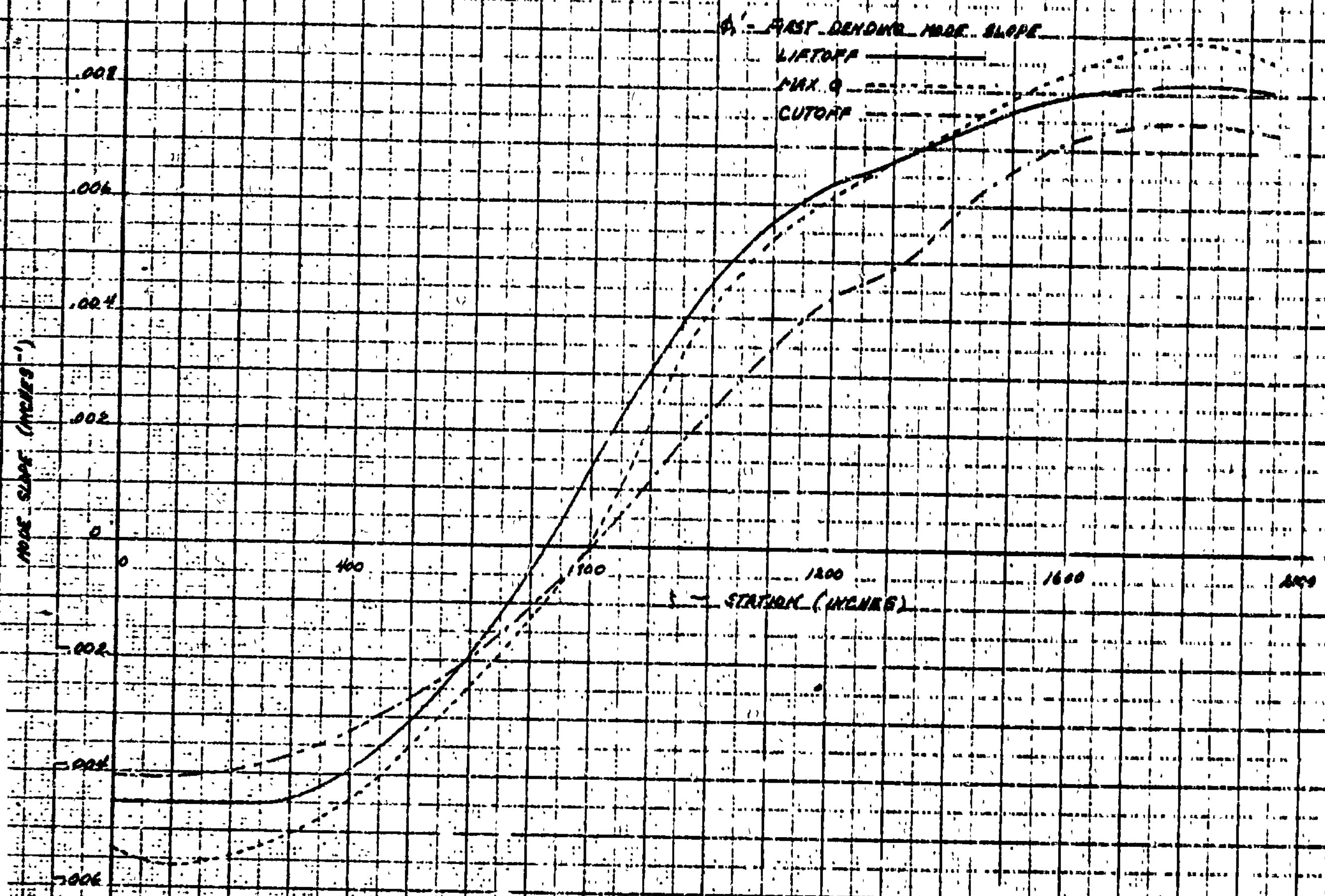
ϕ' - FIRST BENDING MODE SLOPE
LIFTOFF
MAX Q
CUTOFF
.008
.006
.004
.002
0
.002
.004
.006
MODE SLOPE (INCHES^{-1})
0
400
1200
1600
STATION (INCHES)

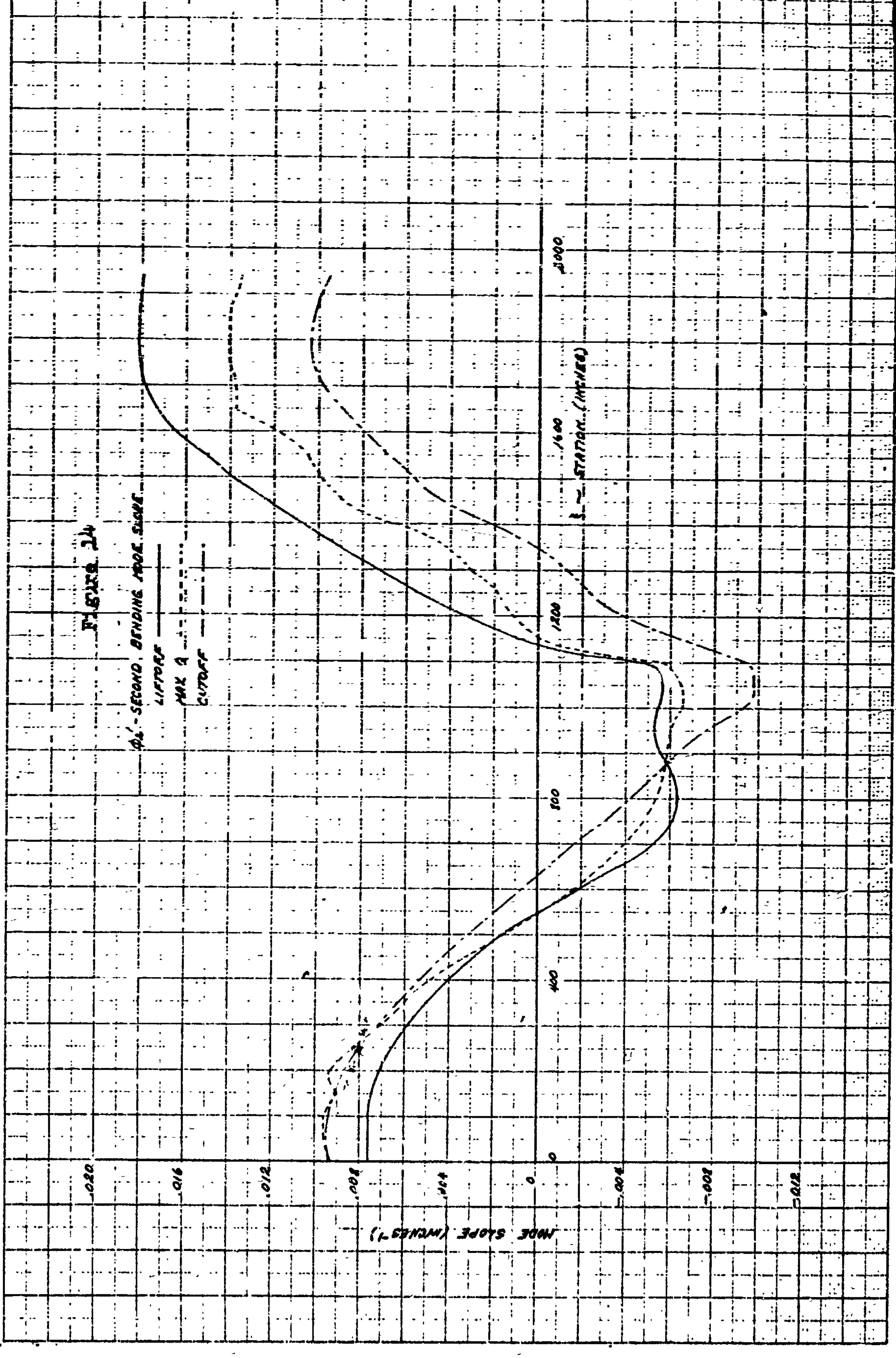
Figure 24
φ2' - SECOND BENDING MODE SLOPE
LIFTOFF
MAX Q
CUTOFF
ℓ ~ STATION (INCHES)
0
400
800
1200
1600
2000
MODE SLOPE (INCHES⁻¹)
.020
.016
.012
.008
.004
0
-.004
-.008
-.012

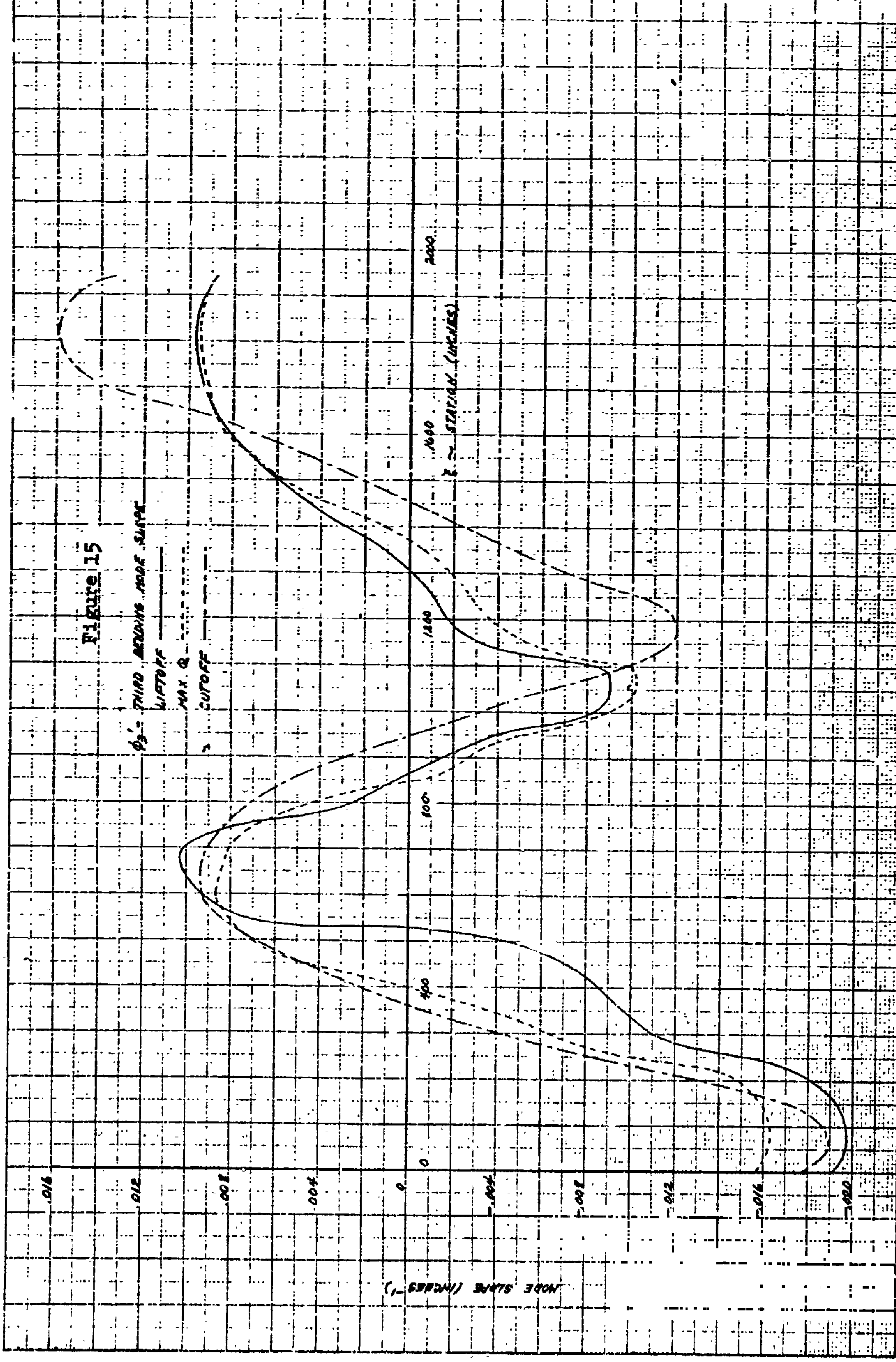
φ3' = THIRD BENDING MODE SLOPE
LIFTOFF
MAX Q
CUTOFF
0
400
800
1200
1600
2000
X ~ STATION (INCHES)
.016
.012
.008
.004
0
-.004
-.008
-.012
-.016
-.020
MODE SLOPE (INCHES⁻¹)

Figure 15

5.5 Analog Computer Mechanization

The diagrams of the analog computer mechanization of the Saturn C-1 missile dynamics used in the study of the adaptive digital bending compensation control system are contained in this section. A discussion of the check procedure used to verify the analog computer mechanization is also included.

Figures 16 and 17 are the mechanization diagrams of the missile dynamics. The equations of the missile dynamics used for the computer mechanization can be found in Section 5.1. These equations were mechanized as listed, with the exception that the attitude rate sensor dynamics and the attitude position sensor dynamics were neglected.

Since this was a study of the flexible body dynamics, the simulation was scaled for a small signal study and, therefore, a linear actuator model was used. This is a conservative approach since, if actuator rate limiting is included, smaller bending mode amplitudes will result than if this limiting is included for a large disturbance input, such as a wind shear disturbance.

In this portion of the study, only the missile configuration corresponding to the flight condition at the time of maximum dynamic pressure was simulated. The coefficients of the equations mechanized are given in Section 5.6 for this flight condition.

The control law used, disregarding the bending compensation provided by the adaptive system, was

$$\delta_c = - a_o \left[\theta_p + \frac{a_1}{a_o} \dot{\theta}_R \right].$$

A detailed check procedure was used to verify the analog computer mechanization of the missile dynamics. A static check of the mechanization was made by applying initial conditions to all of the integrators and reading the values of all the computer variables (outputs of all of the amplifiers). These were compared with precomputed values and satisfactory agreement was obtained.

Dynamic checks of the computer mechanization were made by recording the response of the control system to a step attitude command input. For this check, the digital computer was not used; therefore, the continuous system response was recorded. This time response was compared with one obtained from a digital computer computation of the closed loop response of the system described by the equations listed in Section 5.1, and the results agreed.

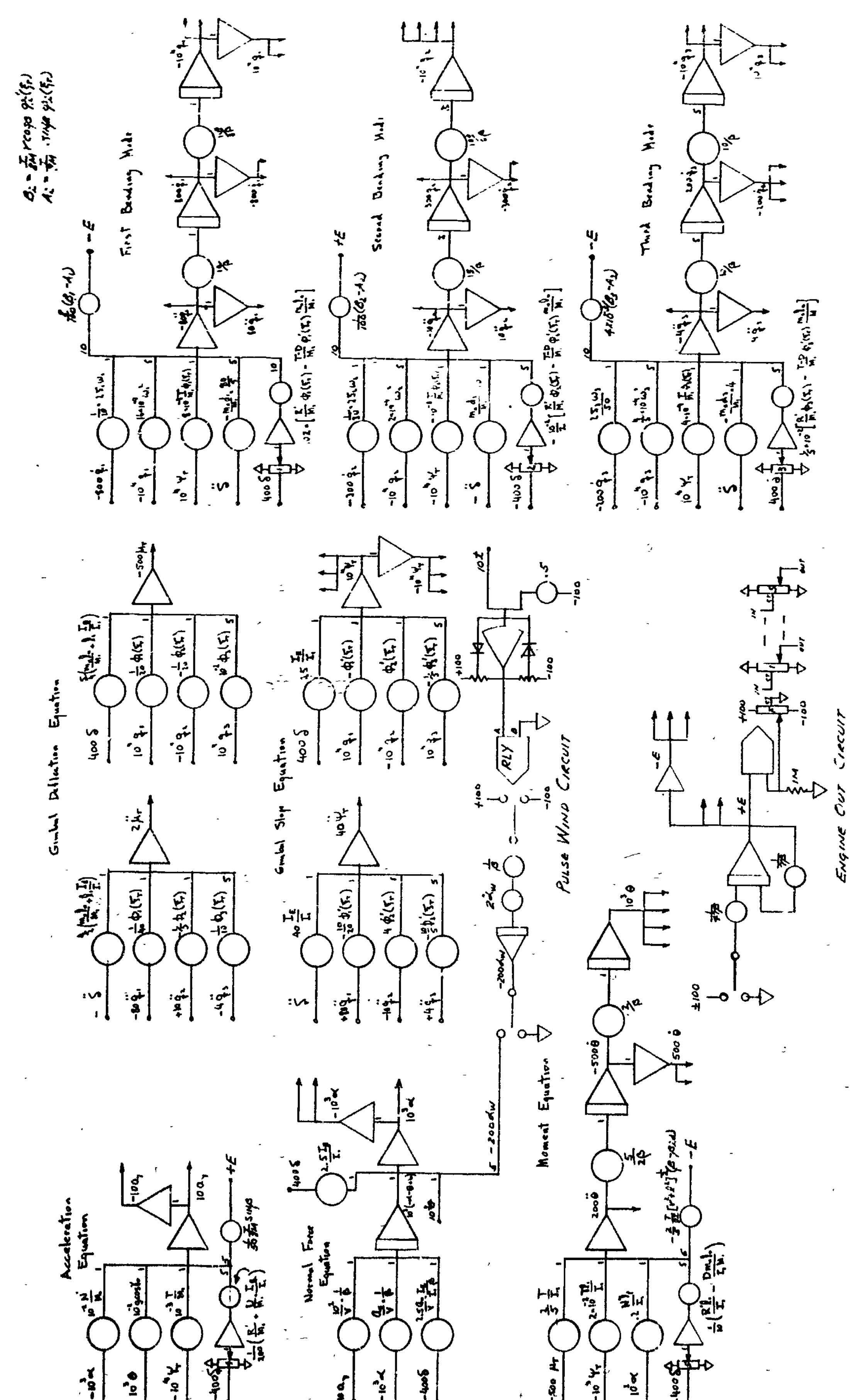

Figure 16
Missile Dynamics Computer Mechanization Diagram (Sheet 1)

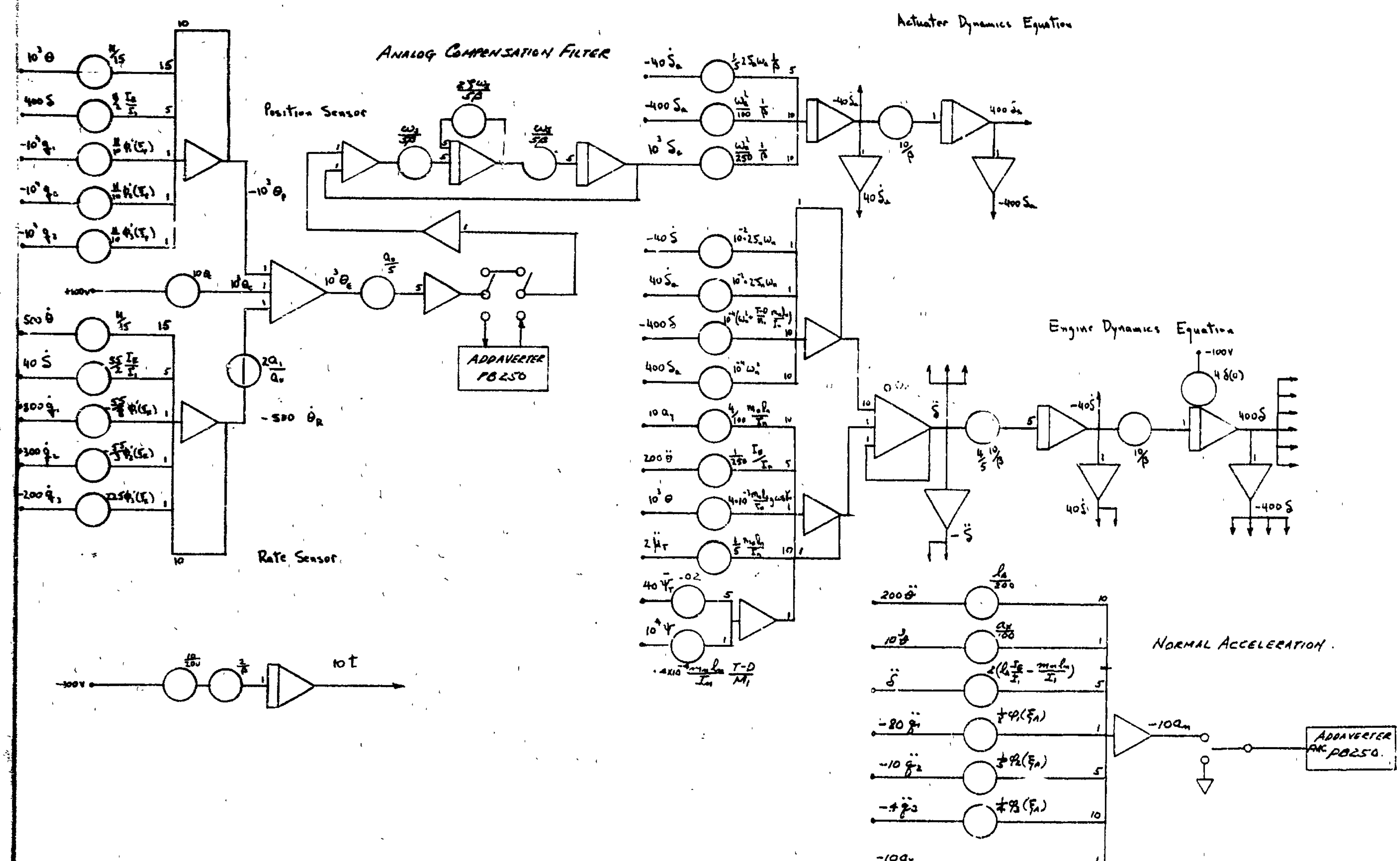

Figure 17
Missile Dynamics Computer Mechanization Diagram (Sheet 2)

5.6. Table of Computed Coefficients (At time of maximum dynamic pressure)

N'/M_1	29.3683932	ft/sec^2
$g \cos \gamma_o$	27.6470293	ft/sec^2
$DI_E/M_1 I_1$	.0098052749	ft/sec^2
T/M_1	73.49621	ft/sec^2
R'/M_1	36.748105	ft/sec^2
$1/V$	.0006958942	sec/ft
a_x/V	.0258729534	sec^{-1}
$a_x I_E/VI_1$	.000029261692	sec^{-1}
I_E/I_1	.00113097609	sec^{-1}
$N' l_p/I_1$	2.4540561	sec^{-2}
$D m_n l_n/I_1 M_1$	.000231405244	sec^{-2}
T/I_1	.0866342	ft^{-1}sec^{-2}
$T l_1/I_1$	3.2284235	sec^{-2}
$R' l_1/I_1$	1.6142118	sec^{-2}
$m_n l_n/M_1$	.022643442	ft
$l_1 I_E/I_1$	.042145824	ft
$\phi_1(\xi_T)$	.97378299	
$\phi_2(\xi_T)$	-1.157848	
$\phi_3(\xi_T)$	1.864179	
$\phi_1'(\xi_T)$	-.067165679	ft^{-1}
$\phi_2'(\xi_T)$	.11517660	ft^{-1}
$\phi_3'(\xi_T)$	-.19540404	ft^{-1}
$2\zeta_1\omega_1$	.13126419	sec^{-1}
$2\zeta_2\omega_2$	.31223919	sec^{-1}
$2\zeta_3\omega_3$	.49885549	sec^{-1}
ω_1^2	172.3029	sec^{-2}
ω_2^2	974.93316	sec^{-2}
ω_3^2	2483.568	sec^{-2}
$\frac{T-D}{M_1}\,\phi_1'(\xi_T)\,\frac{m_n l_n}{M_1}$	-.098592116	ft/sec^2
$\frac{T-D}{M_1}\,\phi_2'(\xi_T)\,\frac{m_n l_n}{M_1}$	.1690570695	ft/sec^2
$\frac{T-D}{M_1}\,\phi_3'(\xi_T)\,\frac{m_n l_n}{M_1}$	-.2868324729	ft/sec^2

5.6 Table of Computed Coefficients (At time of maximum dynamic pressure) - Cont.

$T\phi_1(\xi_T)/M_1$	71.569359	ft/sec^2
$T\phi_2(\xi_T)/M_1$	-85.097438	ft/sec^2
$T\phi_3(\xi_T)/M_1$	37.01009	ft/sec^2
$m_n d_1/M_1$	-.029817968	ft
$m_n d_2/M_1$	.039538624	ft
$m_n d_3/M_1$	-.064811241	ft
$R'\phi_1(\xi_T)/M_1$	35.784679	ft/sec^2
$R'\phi_2(\xi_T)/M_1$	-42.548719	ft/sec^2
$R'\phi_3(\xi_T)/M_1$	68.505044	ft/sec^2
$2\zeta_n\omega_n$	8.7916666	sec^{-1}
ω_n^2	3943.8399	sec^{-2}
$m_n l_n/I_n$	.19578125	ft^{-1}
l_E/I_n	8.2957880	
$m_n l_n g\cos\gamma_o/I_n$	5.41276996	sec^{-2}
$(T-D)m_n l_n/M_1 I_n$	12.691806	sec^{-2}
$\phi_1'(\xi_R)$	-.007533599	ft^{-1}
$\phi_2'(\xi_R)$	-.05770295	ft^{-1}
$\phi_3'(\xi_R)$	.08320151	ft^{-1}
$\phi_1'(\xi_p)$	.10202856	ft^{-1}
$\phi_2'(\xi_p)$	.19171396	ft^{-1}
$\phi_3'(\xi_p)$	.10423876	ft^{-1}
$2\zeta_a\omega_a$	66.670	sec^{-1}
ω_a^2	1190.5	sec^{-2}
a_1/a_o	0.5	
a_o	3.55	

REFERENCES

1. "Wind Speed and Wind Shear Data, Cape Canaveral, Florida", MSFC Memorandum for SATURN Vehicle Dynamics and Control Working Group, 2 February 1961, W. W. Vaughan.

2. "Study of the Control and Dynamic Stability Problem of the SATURN Space Vehicle, Especially the C-1 Configuration", STL Proposal 0353.00, 25 January 1961.